Ion and proton radiography, from prototype to clinical application

Ilaria Rinaldi et al

Lyon 1 University and CNRS/IN2P3, Villeurbanne, France
CREATIS CNRS UMR 5220 – INSERM U1044 – Université Lyon 1 – INSA Lyon
Department of Radiation Therapy and Oncology, Heidelberg University Hospital, Germany
Ludwig Maximilian University, Garching, Germany
Heidelberg Collaboratory for Image Processing, Germany
Department of Radiation Oncology, Massachusetts General Hospital, Boston, USA
Department of Radiation Convergence Engineering, Yonsei University, Wonju, South-Korea
Heidelberg Ion Therapy Center, Germany
GSI Helmholtz Center for Heavy Ion Research, Darmstadt, Germany

Rationale for ion therapy and range verification

<u>Present</u>

- Reduced integral dose (factor ~3)

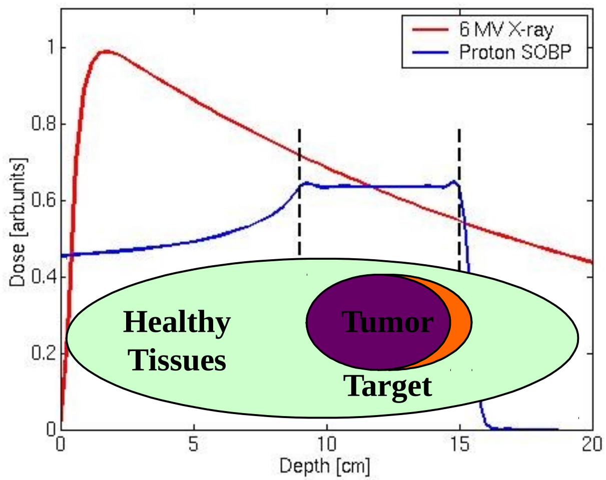

Paganetti AAPM 2012

<u>Future</u>

- Reduction of safety margins
  (dose escalations; higher cure rate)
- Use of new irradiation fields
  (use of sharp distal penumbra of Bragg-peaks)

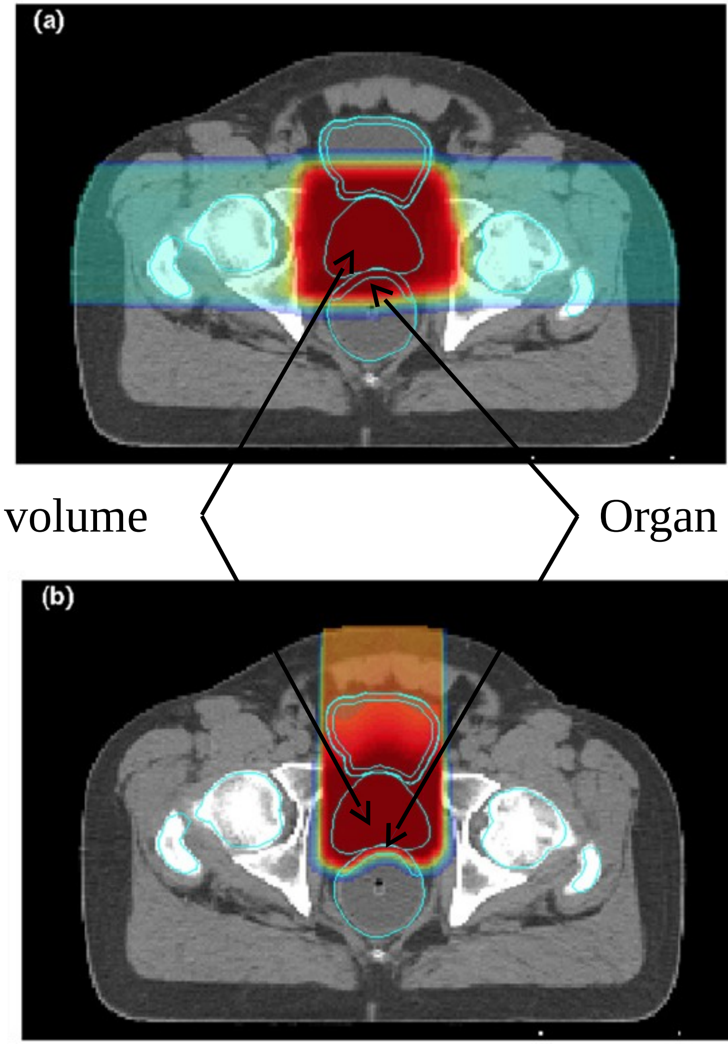

Tumor volume

Organ at risk

Tang et. al. Med.Phys. 2012

How do we reduce range uncertainties?

- In-vivo range verification

PET

Prompt gamma cameras

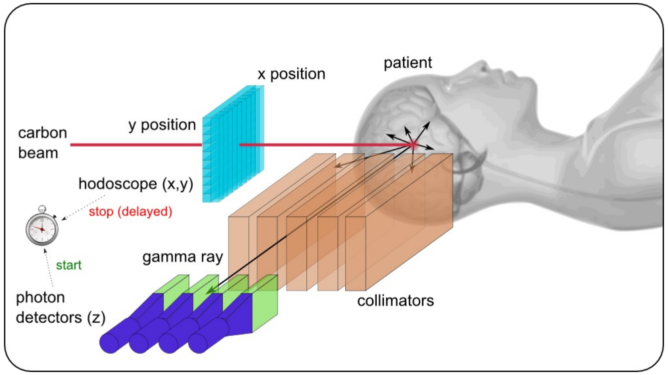

- Increasing accuracy in range prediction

Ion radiography

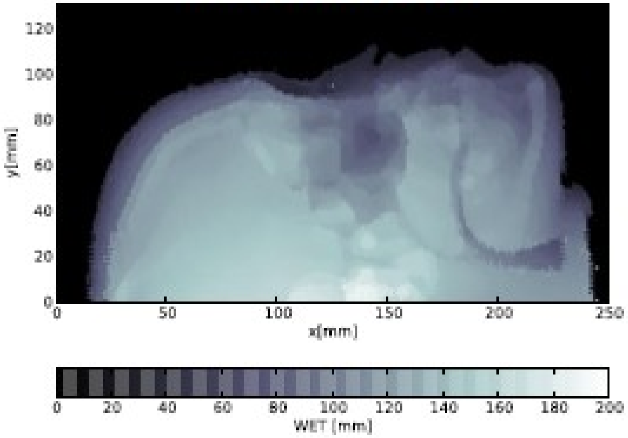

Ion CT

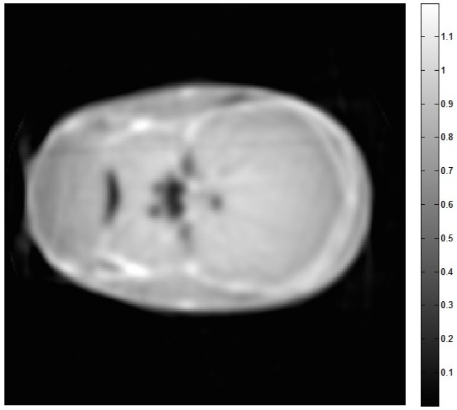

Rationale of Proton Radiography

- Increasing the accuracy of range prediction in the patient by reducing the uncertainties in the conversion curve from HU to proton RSP (~2% range uncertanty in the patient).

Optimization of the HU-RSP based on the minimization of the difference between a proton radiograph and a DRR

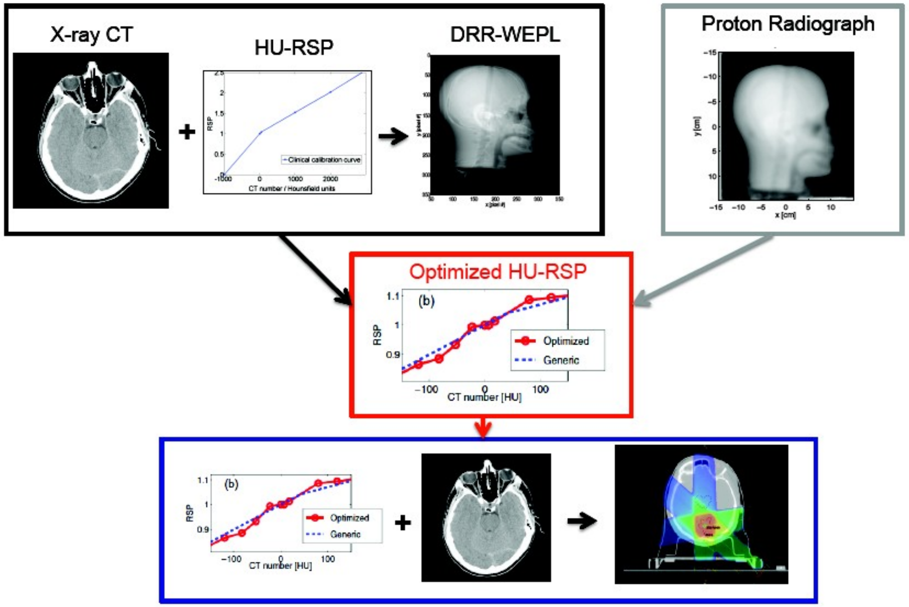

Doolan et.el. PMB 2015
Rinaldi et.al. this AAPM

Proton CT

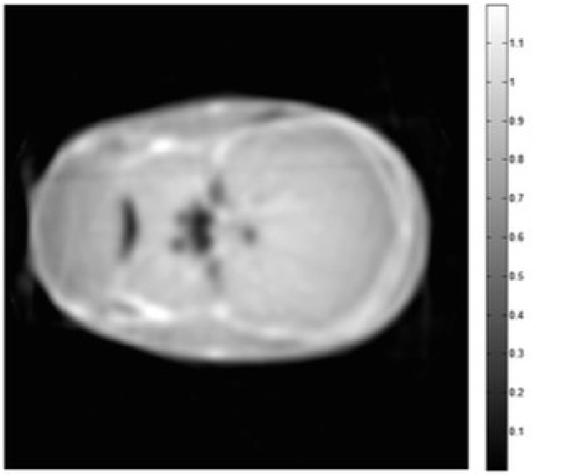

Rinaldi PhD Thesis 2011

<u>Main limitation of proton radiography</u>: poor spatial resolution due proton scattering leading to inaccurate determination of water equivalent thickness (WET) values

-

<u>A potential solution</u>: merging proton radiographs with x-ray radiographs (DRR)

My previous work

Experimental set-up

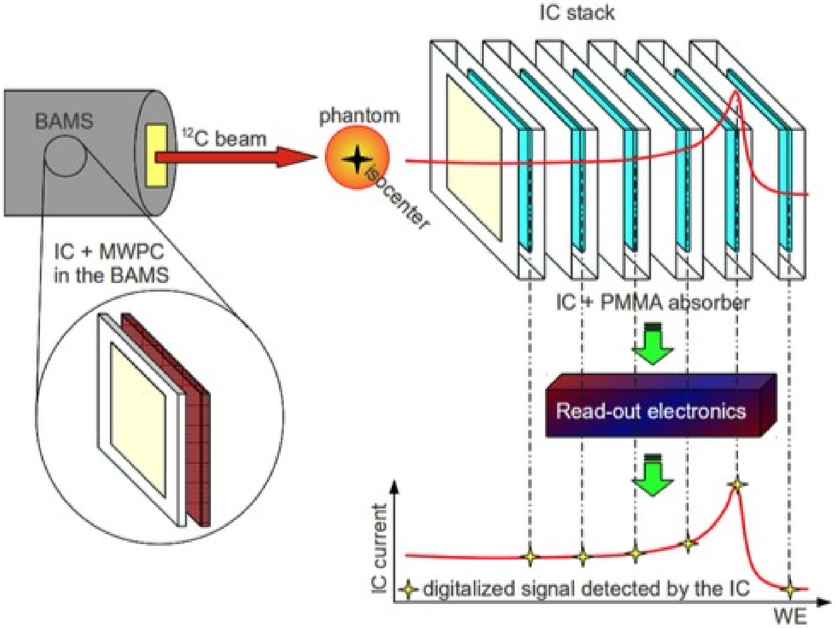

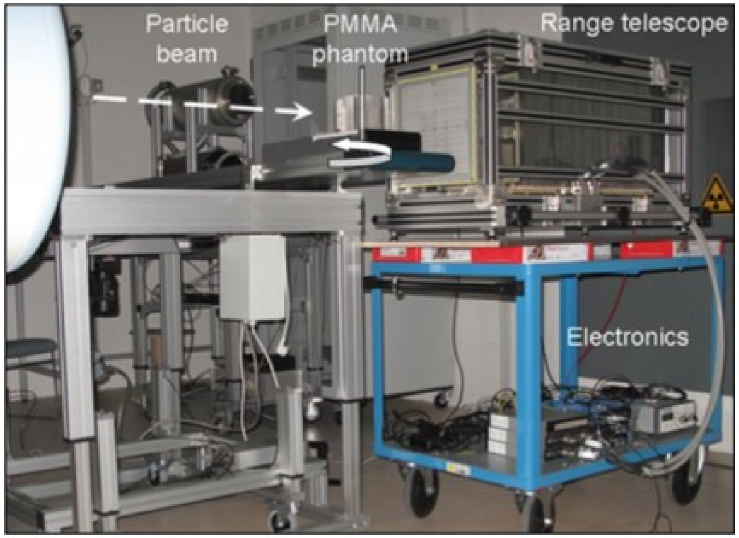

Rinaldi et.al. PMB 2013, 2014a, 2014b

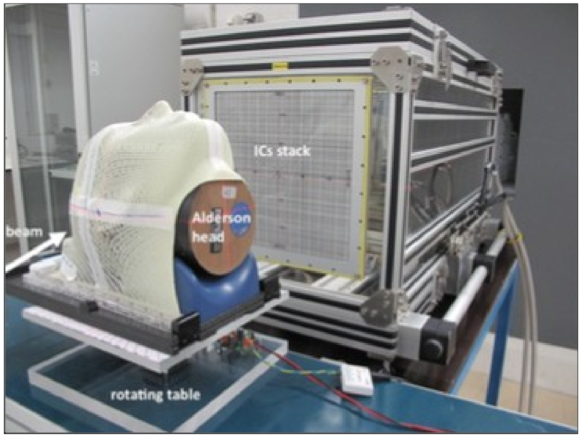

<u>Technical characteristics:</u>

- 61 PPIC 30x30 cm^2
- 3 mm PMMA absorber slabs (3 mm sampling of the BC)
- 2 modules of 32 channels + real time controller
- Active scanning beam delivery system providing transverse information for image reconstruction

Results: Anthropomorphic Alderson head phantom

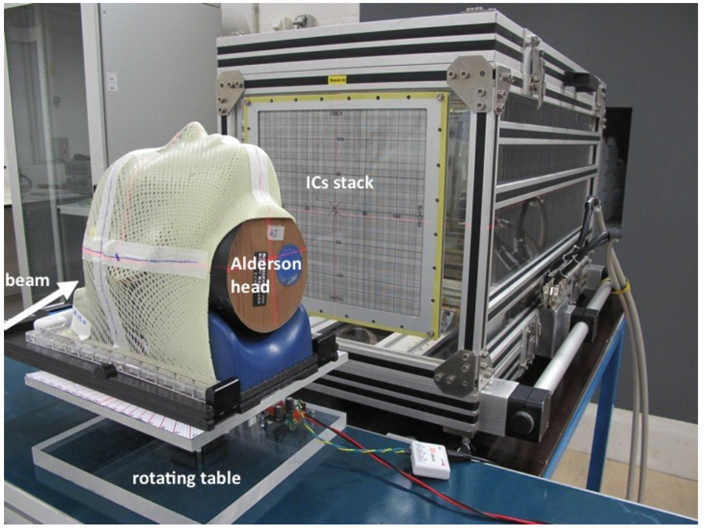

Carbon ion
Energy 313.76 MeV/u
Spot size 3.8 mm FWHM

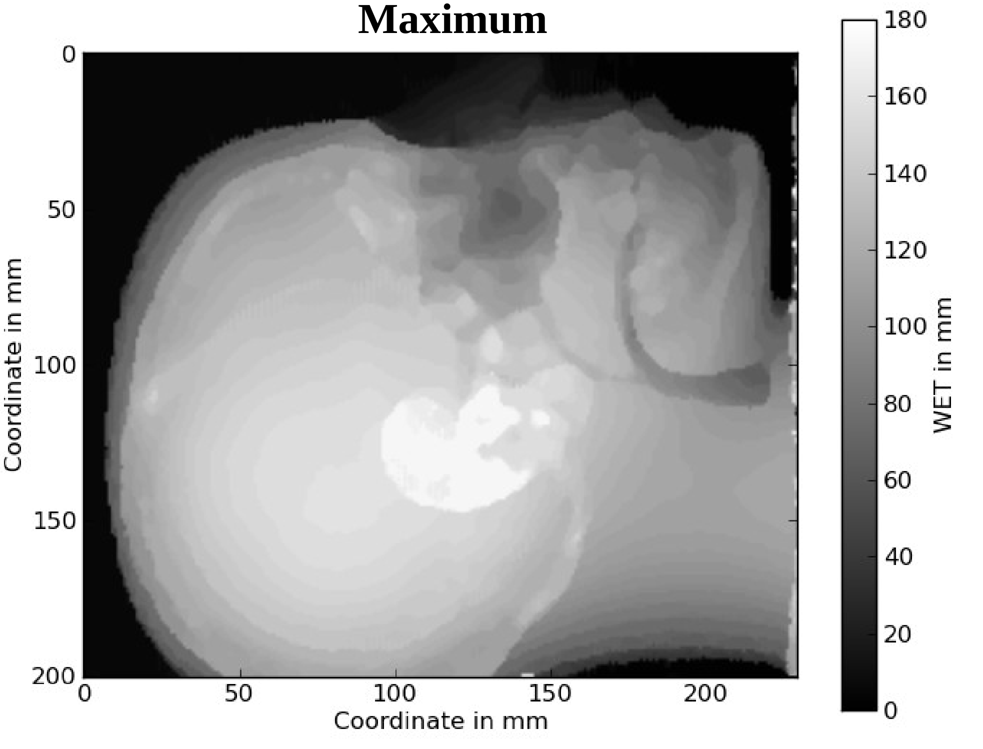

Rinaldi et al., PMB 59 2014, 2015 in press

Results: Anthropomorphic Alderson head phantom

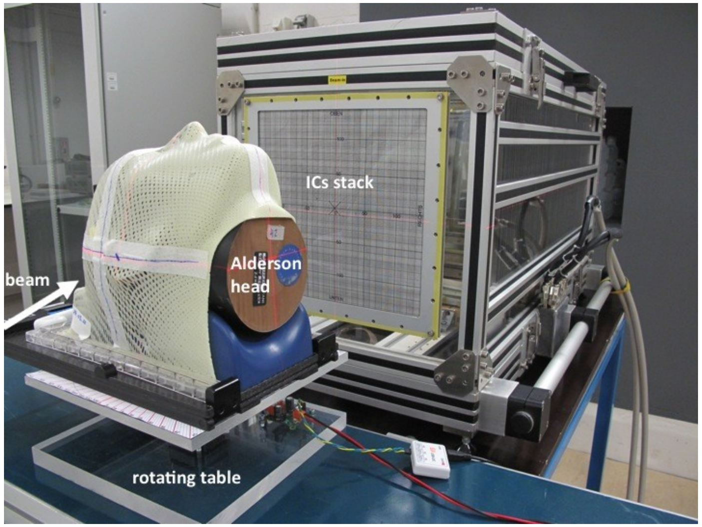

Carbon ion
Energy 313.76 MeV/u
Spot size 3.8 mm FWHM

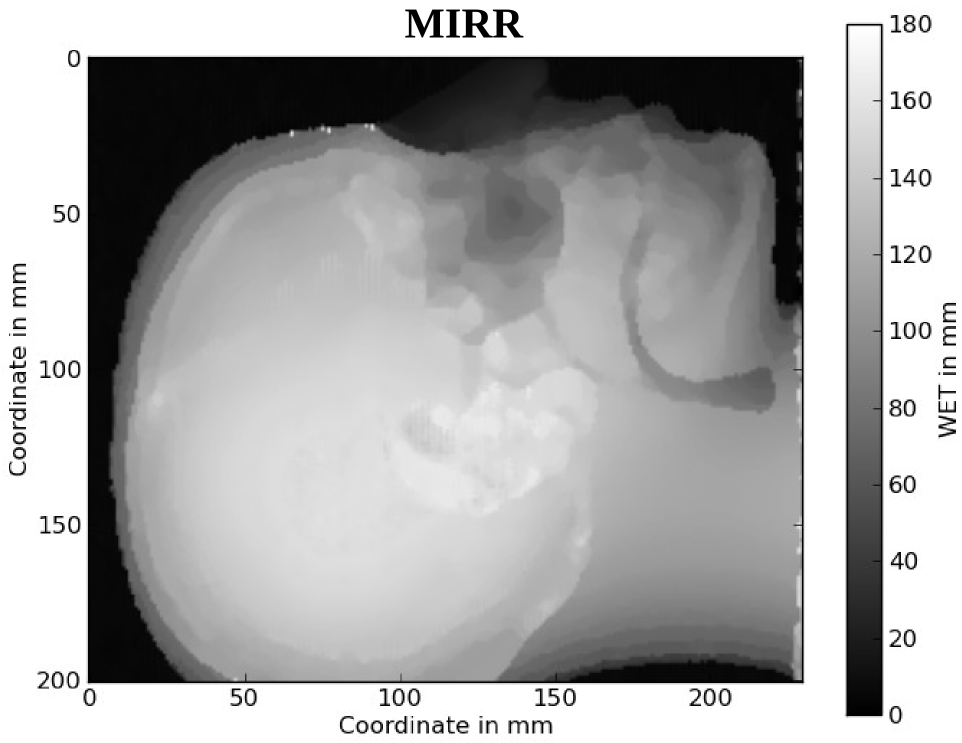

Rinaldi et al., PMB 59 2014, 2015 in press

Results: Anthropomorphic Alderson head phantom

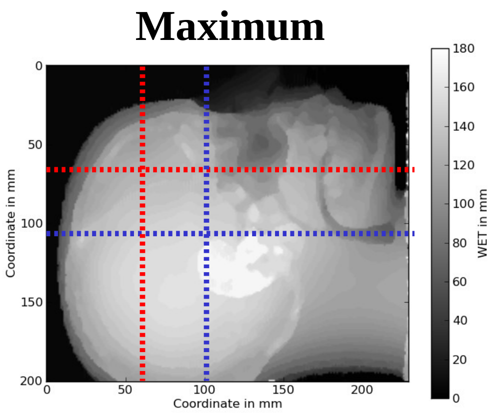

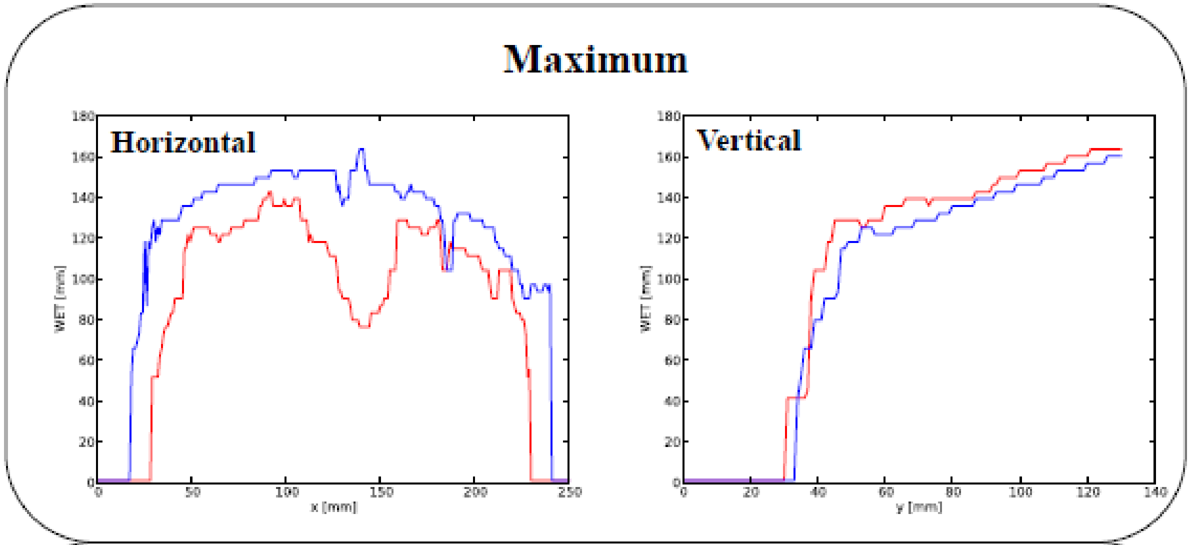

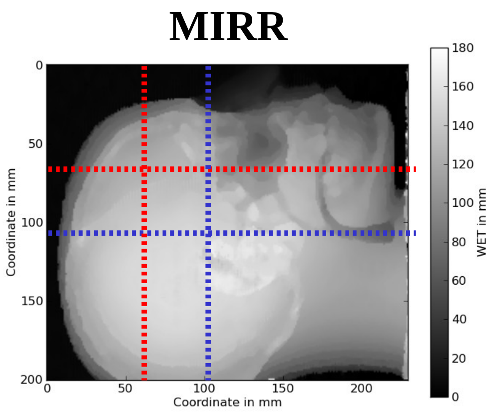

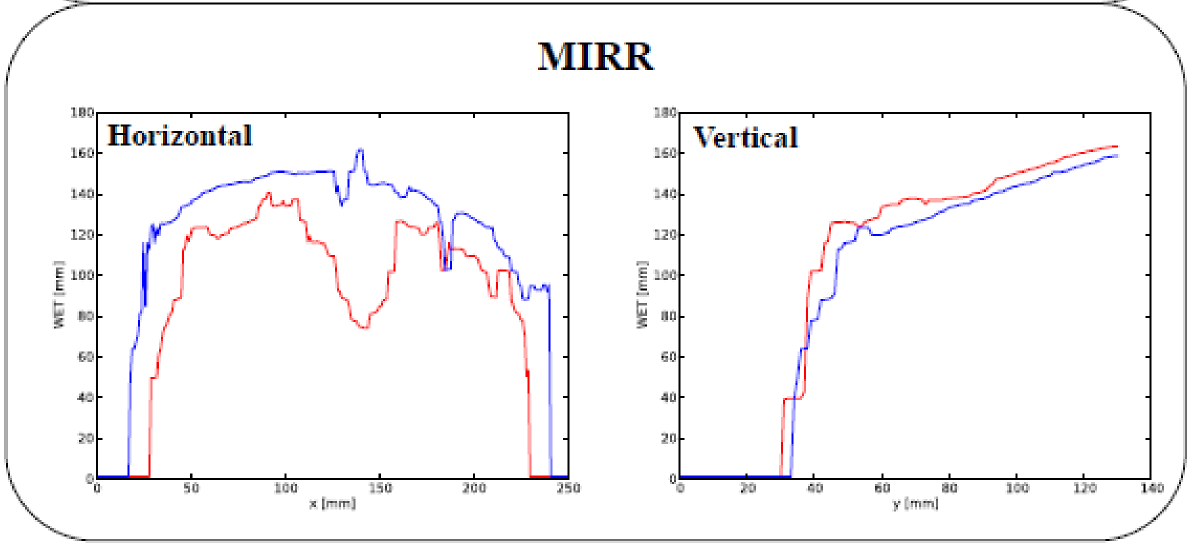

Rinaldi et al., PMB 59 2014, 2015 in press

Results: Anthropomorphic Alderson head phantom

Carbon ion of 313.76 MeV/u

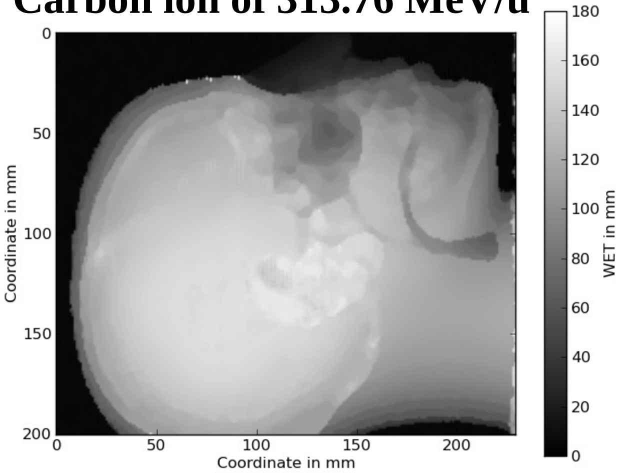

DRR: X-ray of 120 KV

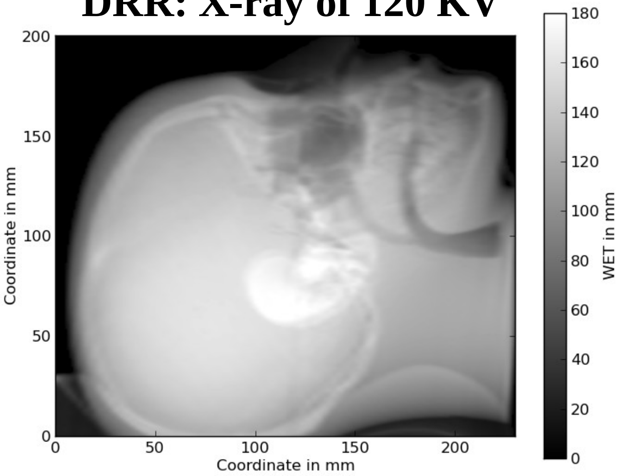

Rinaldi et al., PMB 59 2014, 2015 in press

Results: Anthropomorphic Alderson head phantom

Carbon ion of 313.76 MeV/u

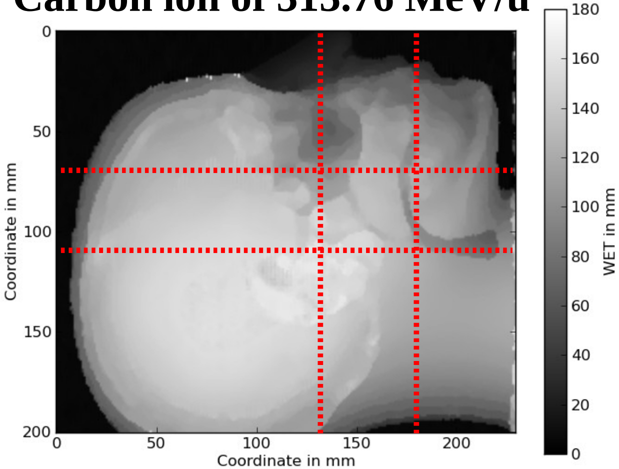

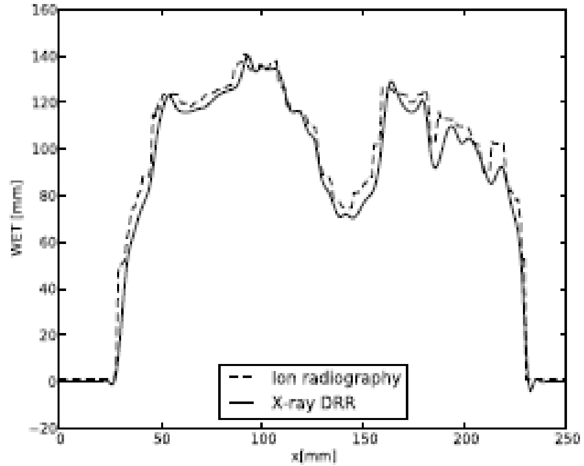

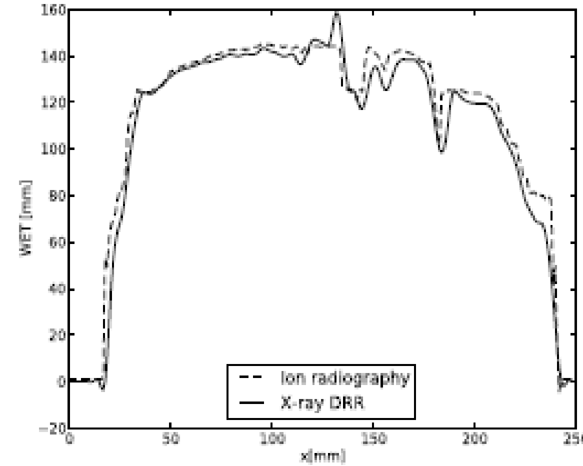

DRR: X-ray of 120 KV

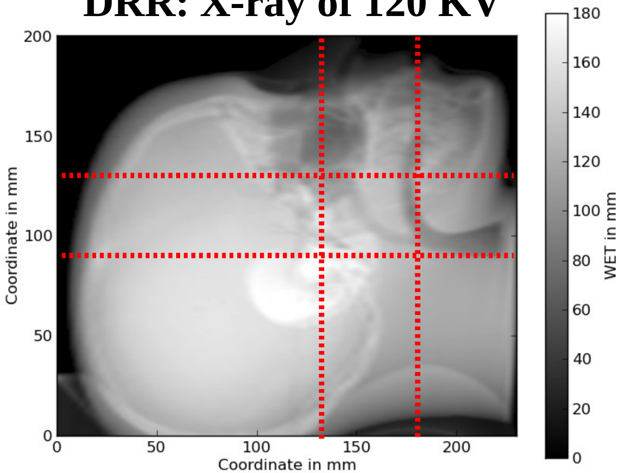

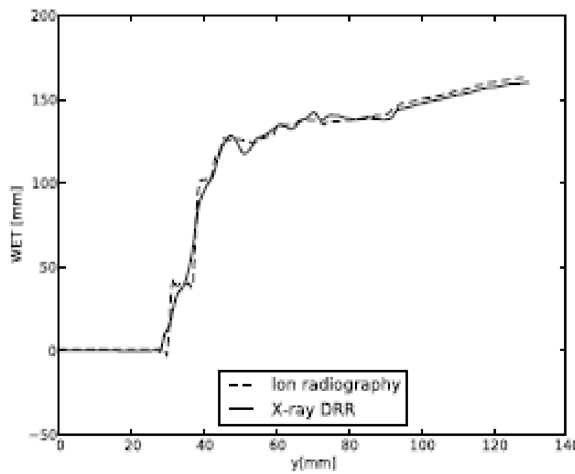

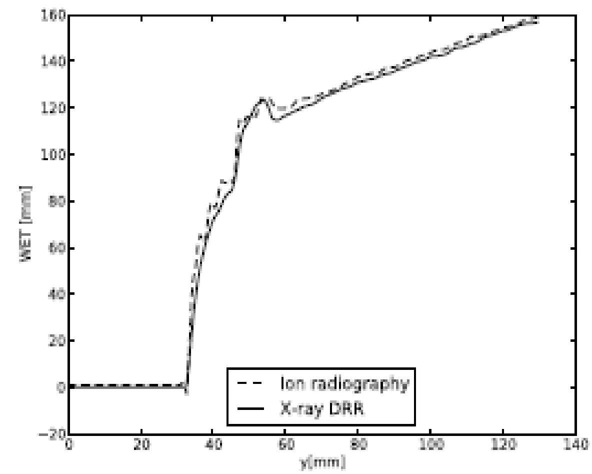

Rinaldi et al., PMB 59 2014, 2015 in press

Distortion and bias of proton radiographies

Proton beam with extended size
passing through lateral inhomogeneity

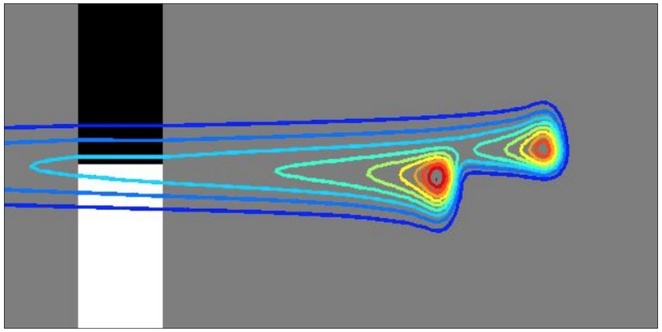

J. Unkelbach MGH

Measured signal in the IC-stack

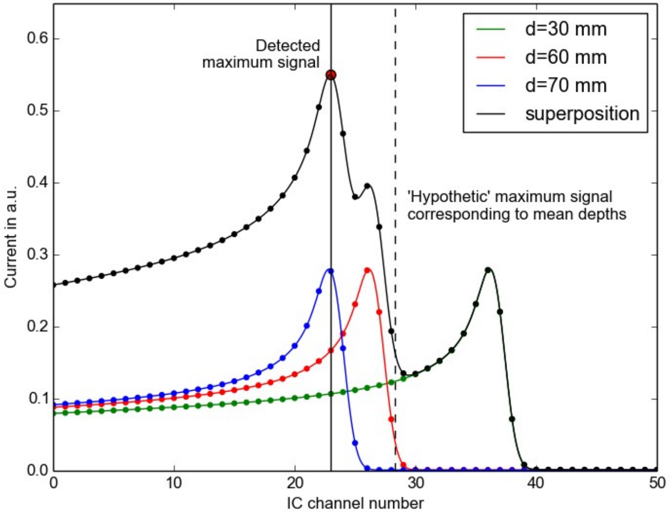

X-ray radiography (DRR)

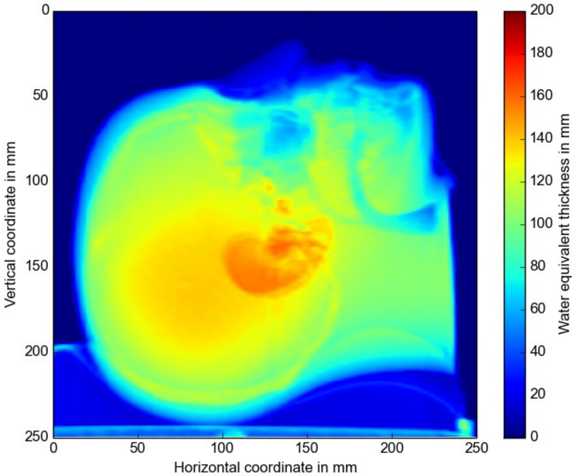

Proton radiography

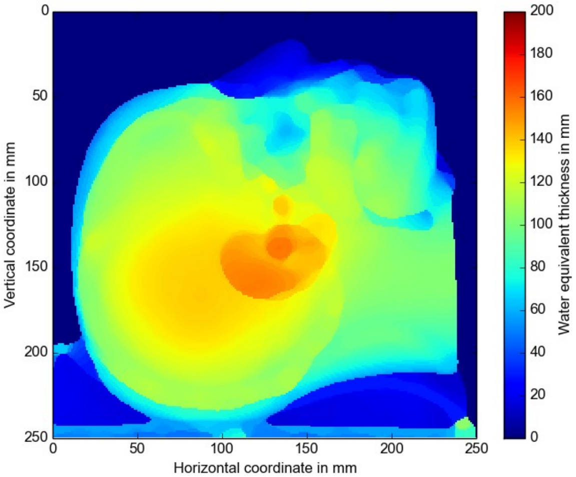

Difference: X-ray – Proton Radiography

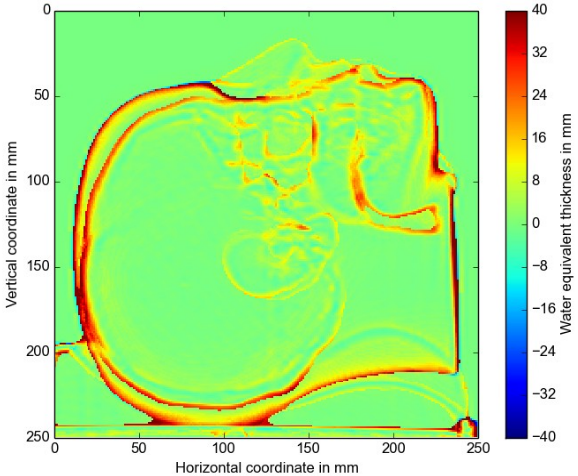

- Thicker regions extend into adjacent thinner regions
- The edges of the object are larger than real

Step 1. Decomposition of measured Bragg-Curves

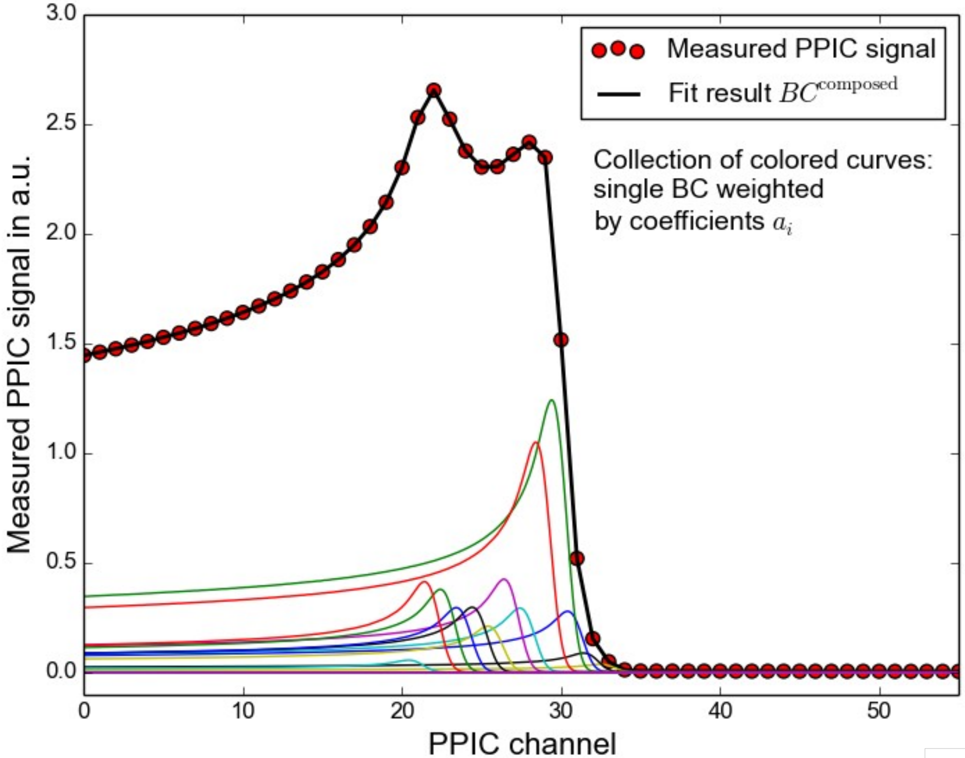

Krah, Rinaldi et al., PMB 2015 in press

Monte Carlo database of Bragg-Curves

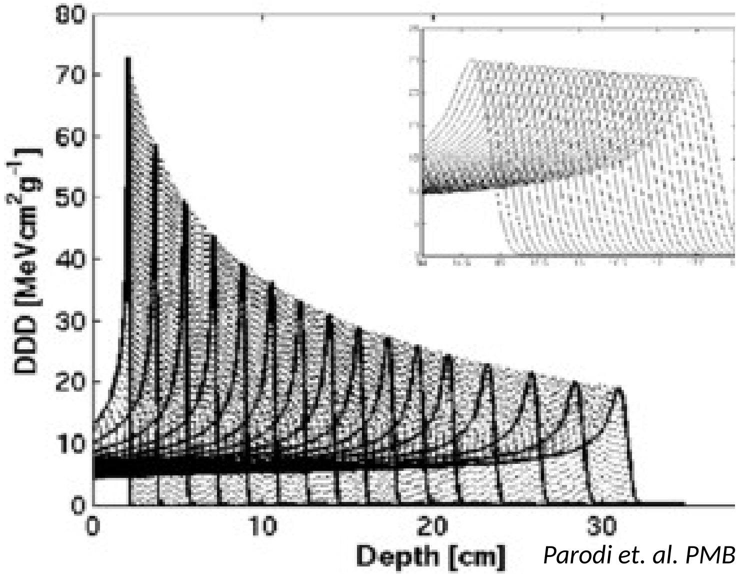

Parodi et. al. PMB 2012

$$BC^{composed}(z_k) = \sum_{i=1}^{M} a_i \; BC_0(z_k + d_i),$$

$$\frac{1}{N}\sum_{k=1}^{N}\left\{BC_p^{meas}(z_k) - BC^{composed}(z_k) - \Psi\right\}^2 \longrightarrow \min,$$

$$D_p = \sum_{i=1}^{M} \tilde{a}_{pi} \cdot d_{pi}.$$

- Measured BC decomposed into a combination of BC from the database

- The sum of constituent BCs best approximate the measured BC

- The weight of each BC determines its relative contribution to the measured BC

- Calculation of the WET as weighted average of the decomposed BC

Step 2. Sub-images

Krah, Rinaldi et al., PMB 2015 in press

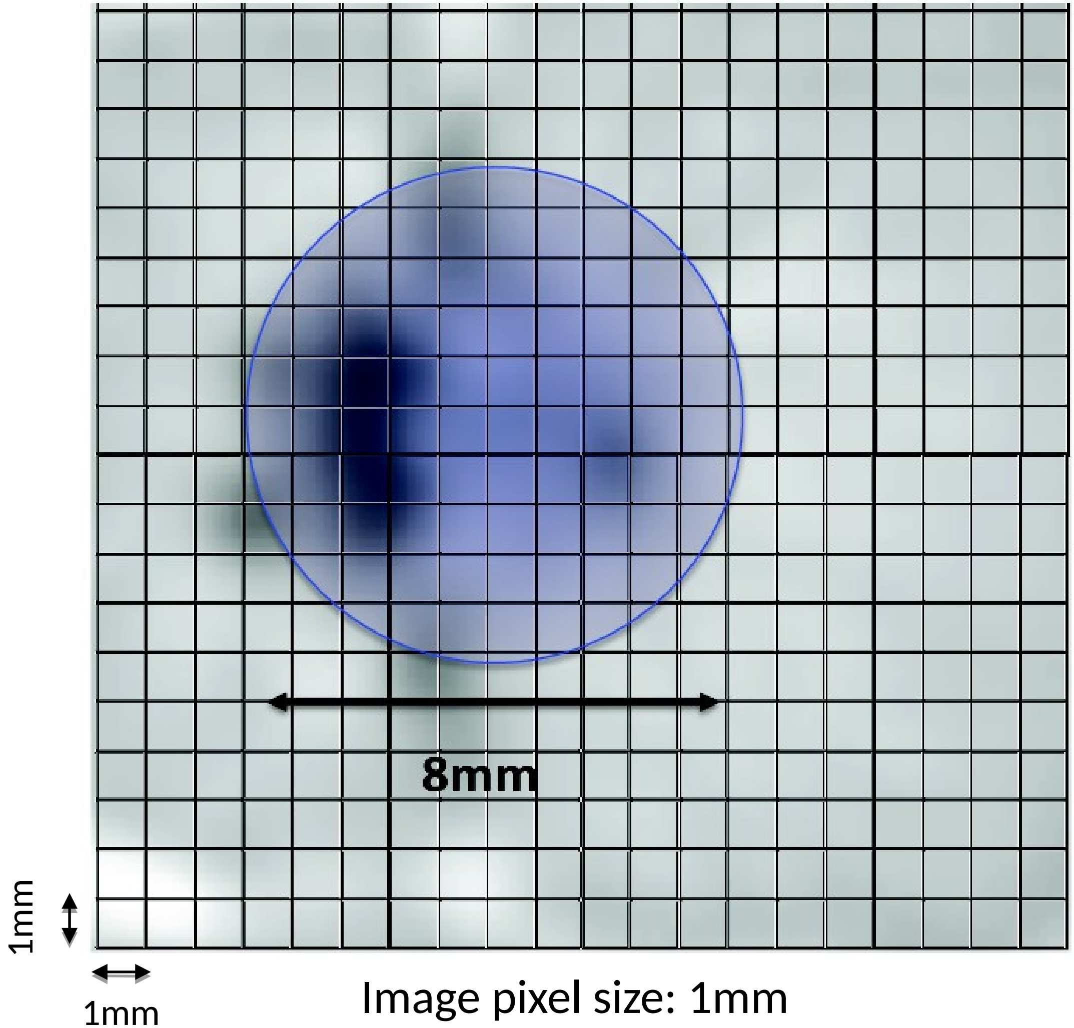

Image pixel size: 1mm
FWHM beam: 8mm
Step-size raster scanning: 1mm
<u>The beam covers multiple pixels</u>

Step 2. Sub-images

Krah, Rinaldi et al., PMB 2015 in press

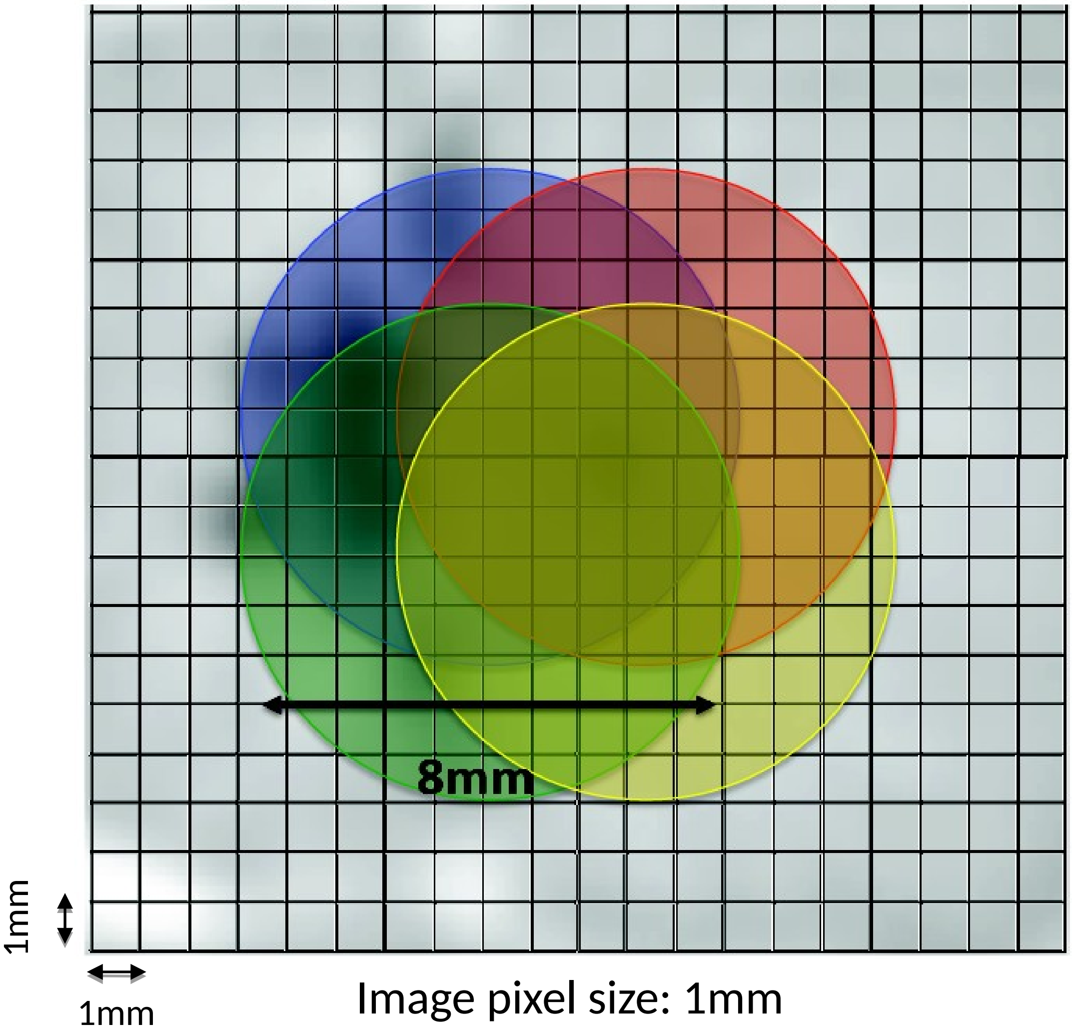

Image pixel size: 1mm
FWHM beam: 8mm
Step-size raster scanning: 1mm

The algorithm exploits the redundant information of overlapping subimages

Step 2. Sub-images

Krah, Rinaldi et al., PMB 2015 in press

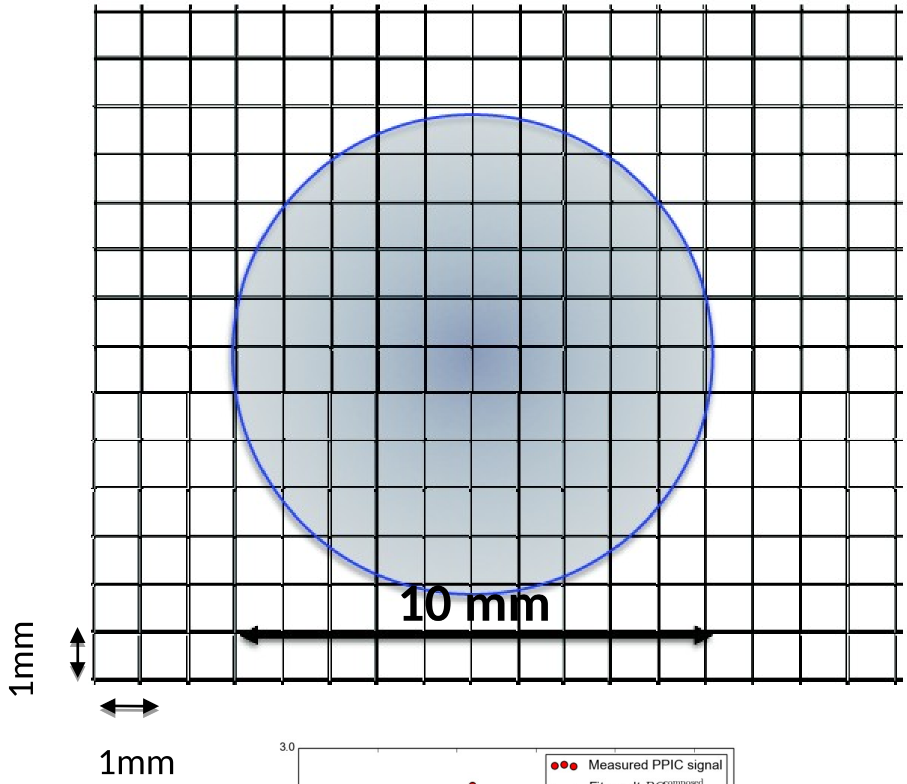

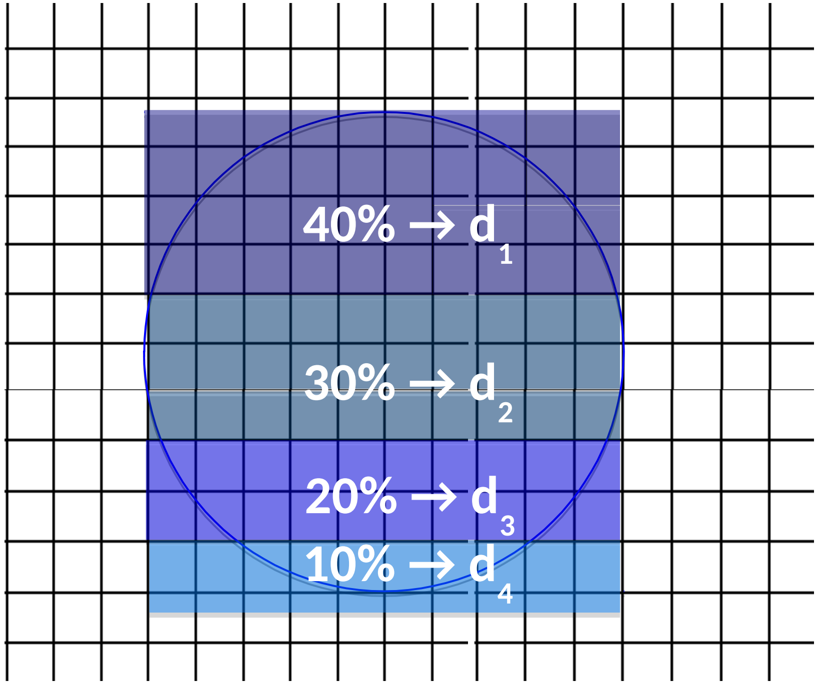

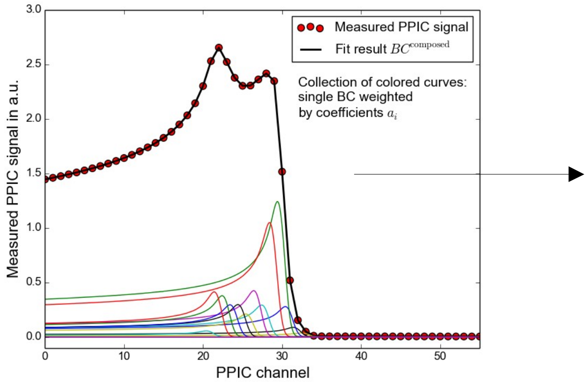

$$D_p = \sum_{i=1}^{M} \tilde{a}_{pi} \cdot d_{pi}.$$

$D_p = 0.4\times d_1 + 0.3\times d_2 + 0.2\times d_3 + 0.1\times d_4$

Measured BC decomposed into 4 constituent Bcs with **thicknesses** d_1, d_2, d_3, d_4 and weights 40%, 30%, 20%, 10%

Step 3. Demosaicing of sub-images

Krah, Rinaldi et al., PMB 2015 in press

Non-optimized proton radiography

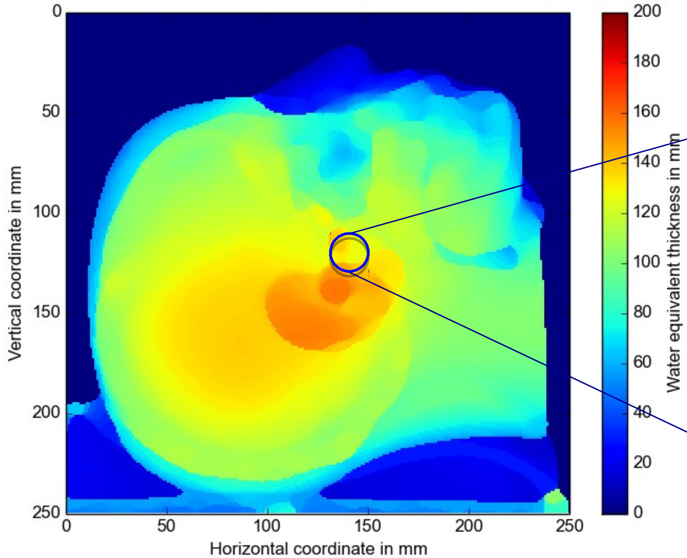

X-ray DRR

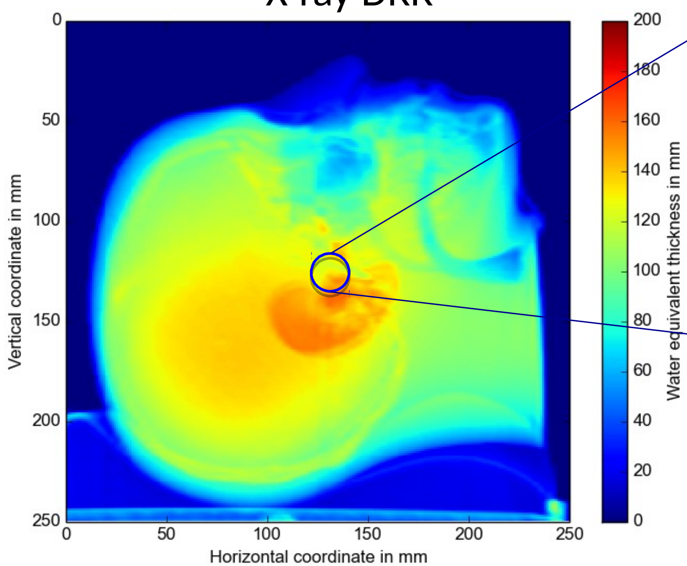

Re-arranged sub-image

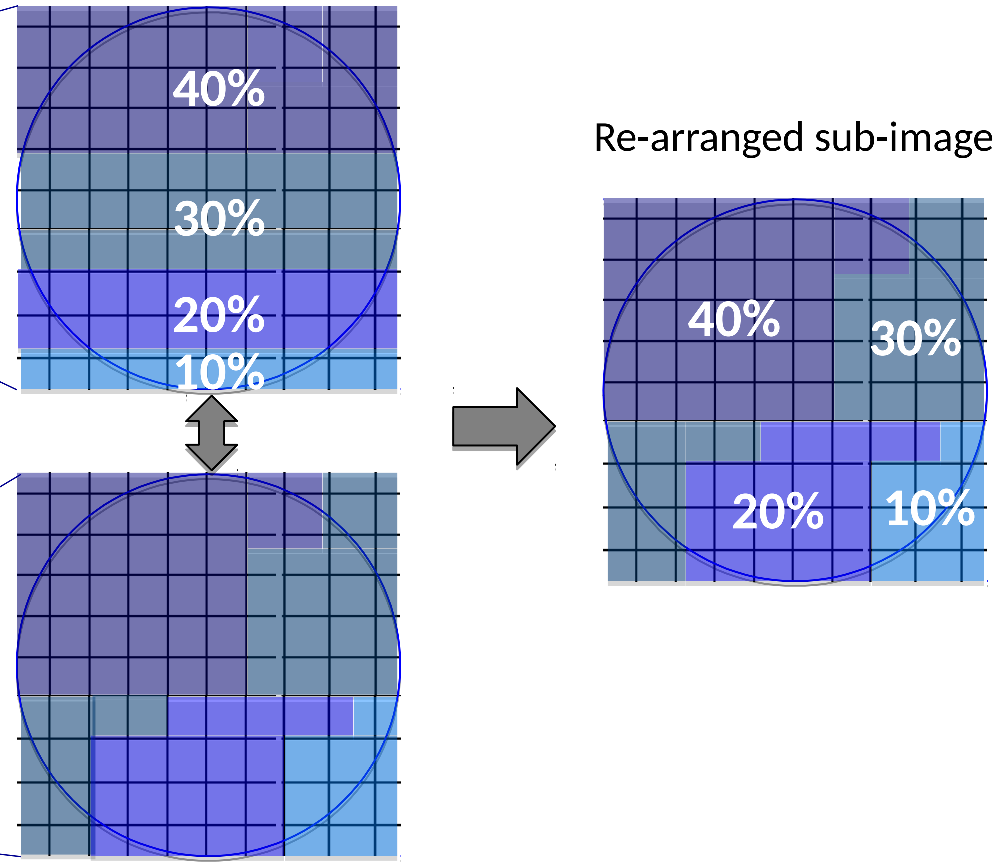

Only the pixel geometric reference is taken from the DRR.
WET values come only from the proton radiography.

Step 4. Averaging over overlapping sub-images

Krah, Rinaldi et al., PMB 2015 in press

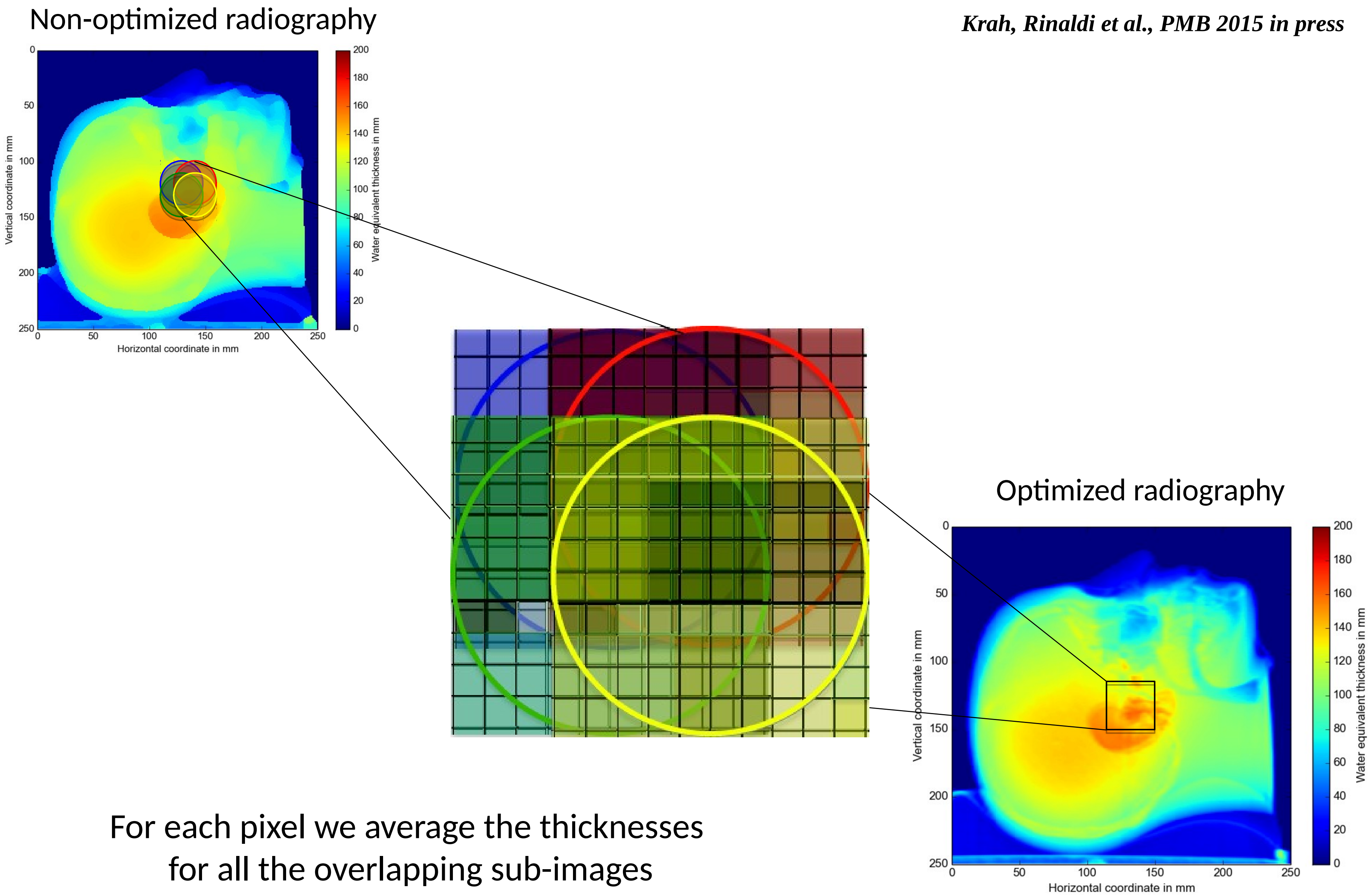

For each pixel we average the thicknesses
for all the overlapping sub-images

Results: Monte Carlo simulated proton radiographies

Krah, Rinaldi et al., PMB 2015 in press

Difference between x-ray DRR and Proton Radiography

Non- Optimized

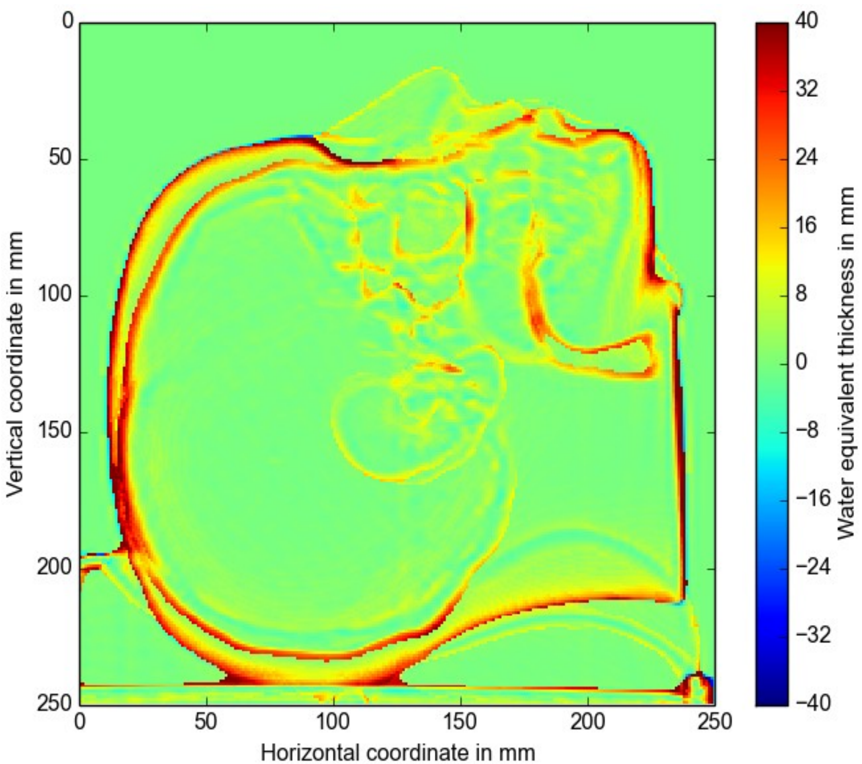

Optimized with DRR

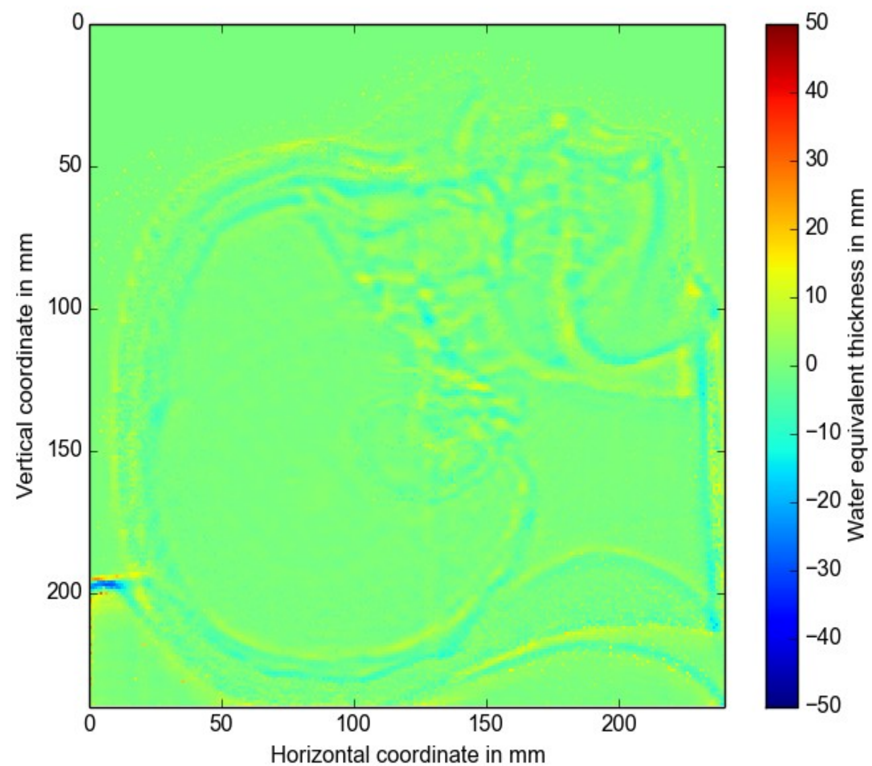

Results: Monte Carlo simulated proton radiographies

Krah, Rinaldi et al., PMB 2015 in press

Non- Optimized

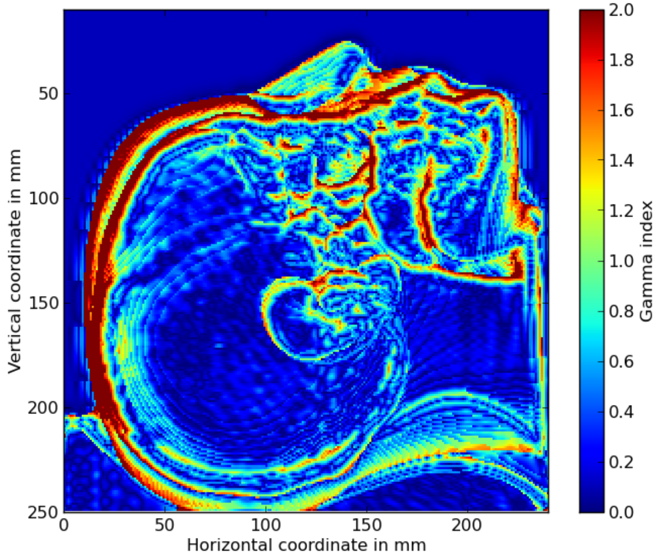

Optimized with DRR

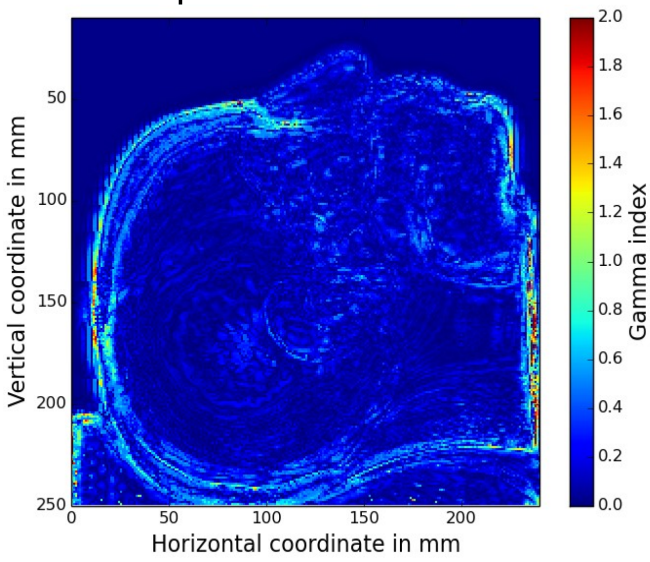

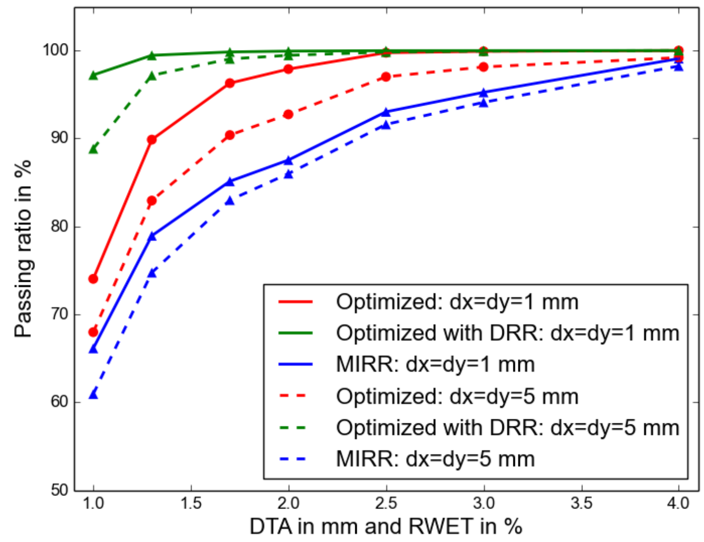

Non optimized

100% passing ratio for 4%-4 mm

Optimized

100% passing ratio for 1.5%-1.5 mm

Results: Experimental proton radiographies

Krah, Rinaldi et al., PMB 2015 in press

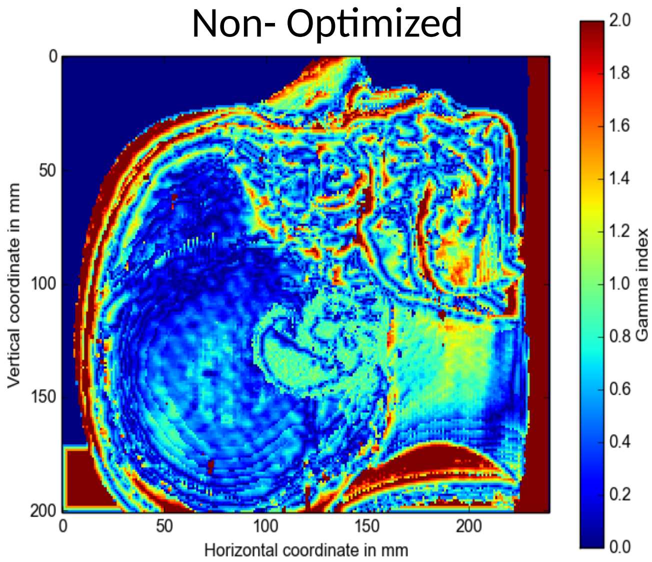

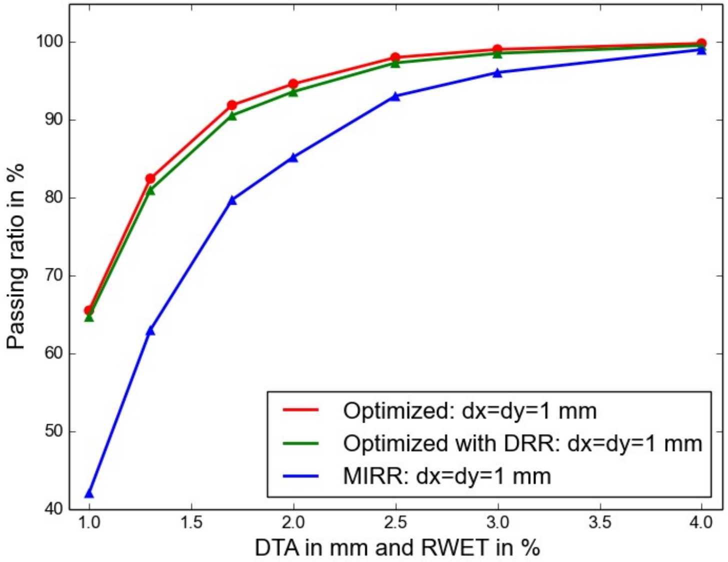

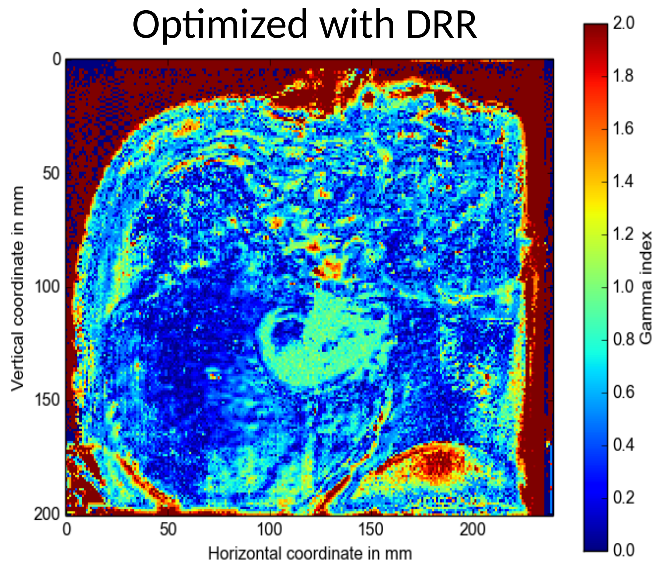

<u>Non optimized</u>

100% passing ratio for 4%-4 mm

<u>Optimized: Co-registered by hand with DRR</u>

100% passing ratio for 2.5%-2.5 mm

No X-ray positioning system in the experimental room at HIT

Results: Reducing the dose by increasing raster scanning steps

Krah, Rinaldi et al., PMB 2015 in press

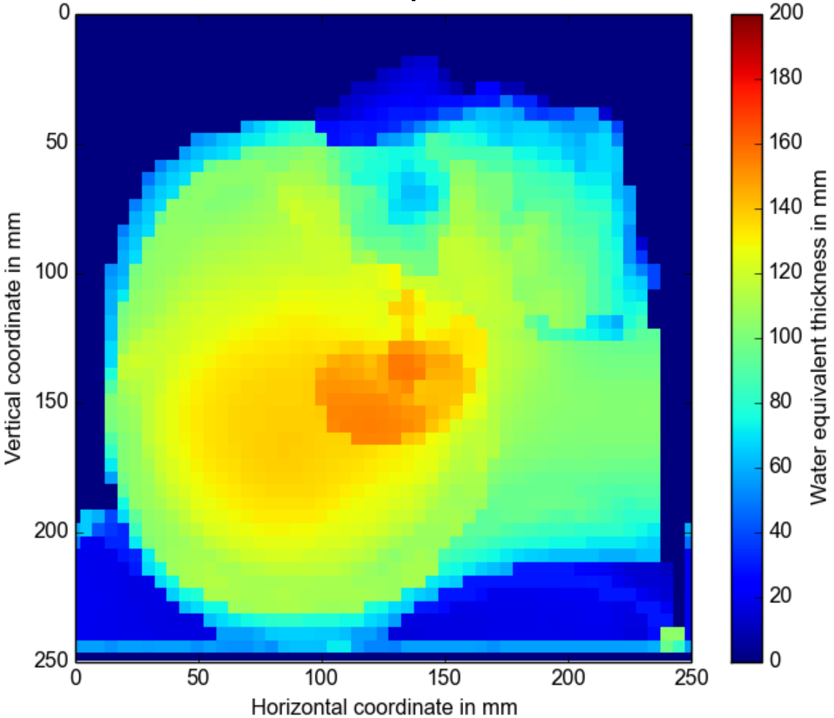

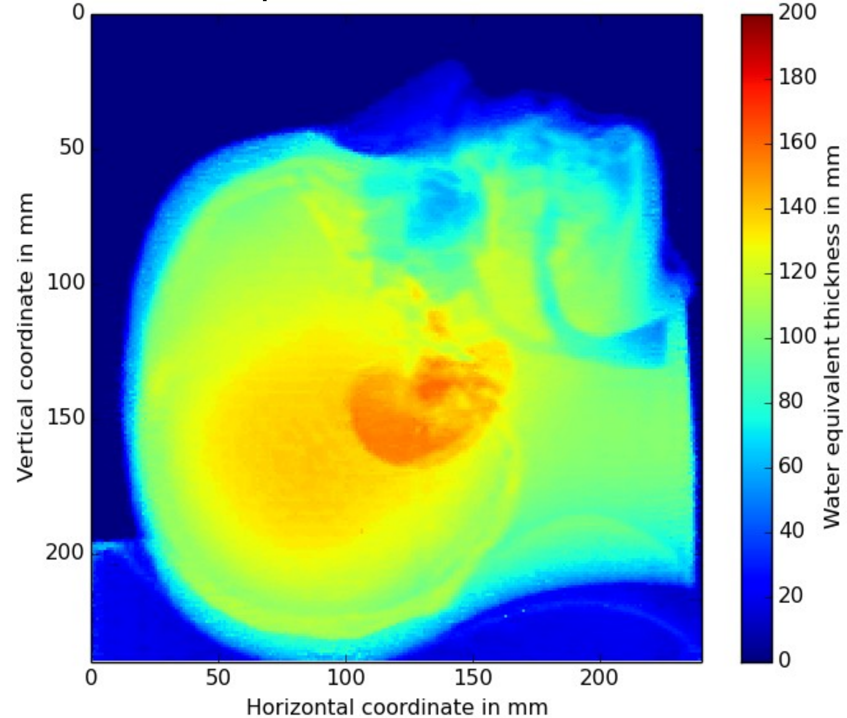

Raster scanning step 5mm → Dose reduction 25 times

0.4 mGy → 0.016 mGy

Conclusions & Perspectives

- We developed an image process algorithm that allows to greatly increase the spatial resolution of proton radiographies

- When precise co-registration with an x-Ray image is available the spatial resolution of the proton radiography becomes comparable to the the one of the x-Ray image

- The algorithm allows to reduce the dose per radiography by increasing the raster scanning steps. A reduction of 25 times the nominal dose (from 0.4mGy to 0.016mGy) still produce images with a fair rendering of anatomical structures

- The algorithm can potential be applied to merge proton-CT and X-ray CT by performing the optimization on each projection

- The algorithm can be adapted to other radiography systems using beams with extended size

Krah, Rinaldi et al., PMB 2015 in press

Work previously done in Lyon

Filtered backprojection proton CT reconstruction along most likely paths

Rit et al., Med Phys 2013

- filtered backprojection (FBP) algorithm

- curved most likely path estimation

- use distance driven binning in order to improve the spatial resolution in proton radiographs. During backprojection, the spatial position of each voxel is translated to a distance to the source and the corresponding radiograph in the binned radiographs is used so that the sharpest binning is selected for objects at the voxel location.

- MC simulated data

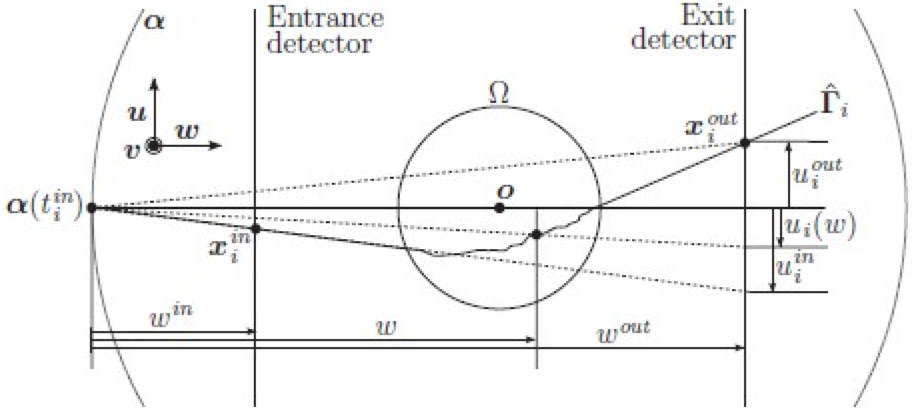

Filtered backprojection proton CT reconstruction along most likely paths

Rit et al., Med Phys 2013

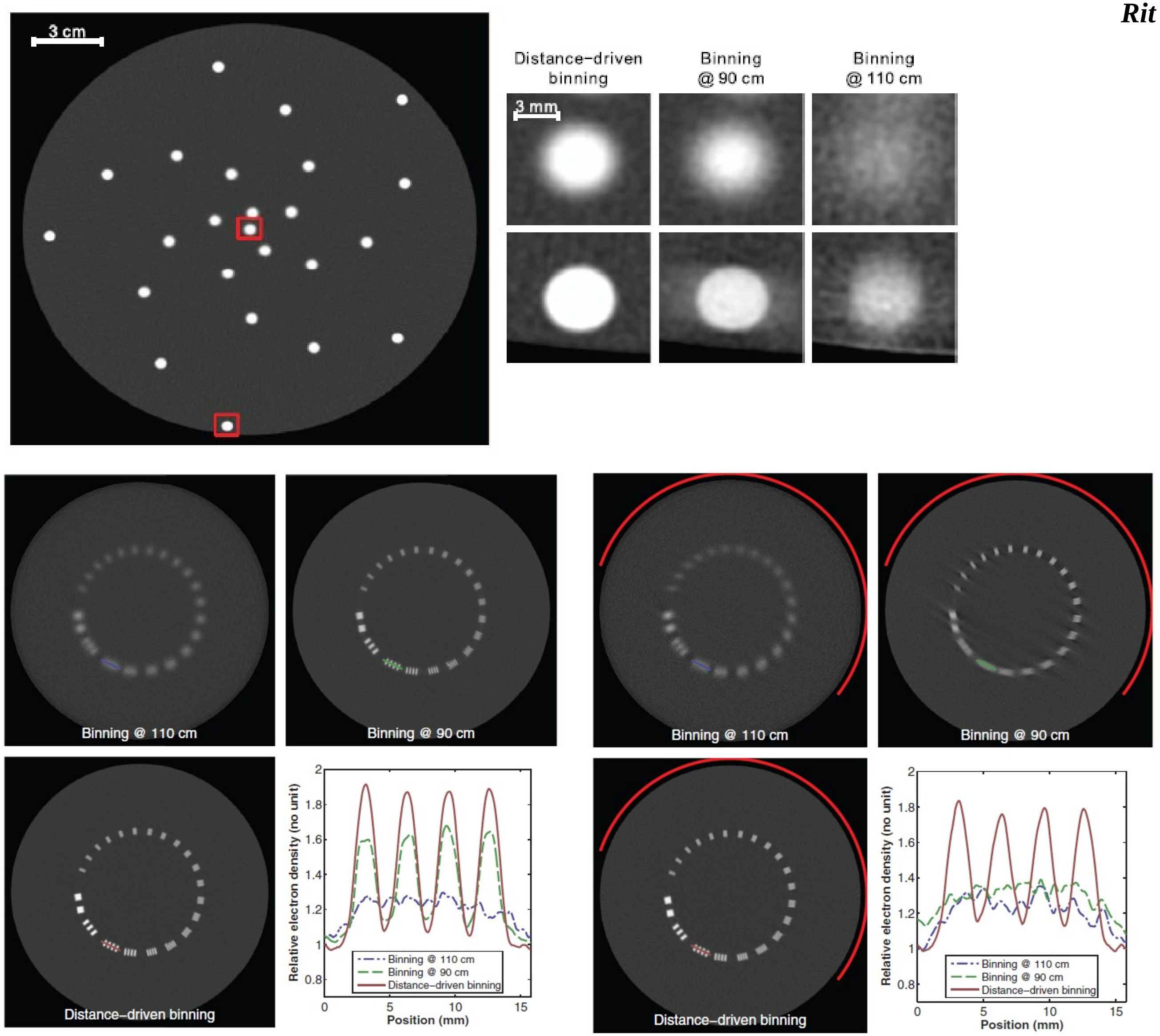

Conclusion

We have developed a filtered-backprojection pCT reconstruction algorithm that takes advantage of the estimation of the most likely path of protons. Improvement in the spatial resolution has been observed on Monte Carlo simulations compared to existing straight-line approximations. The improvement in spatial resolution combined with the practicality of FBP algorithms compared to iterative reconstruction algorithms makes this new algorithm a candidate of choice for clinical pCT.

Monte Carlo Comparison of X-ray and Proton CT for Range Calculations of Proton Therapy Beams

Arbor et al., PMB 2015 in press

- developed a Monte Carlo framework to assess proton CT performances for the main steps of a proton therapy treatment planning, i.e., proton or X-ray CT imaging, conversion to relative stopping power maps based on the calibration of a tissue phantom, and proton dose simulations.

- to quantify the accuracy of patient relative stopping power reconstruction with proton CT and the impact on the prediction of proton ranges for proton therapy.

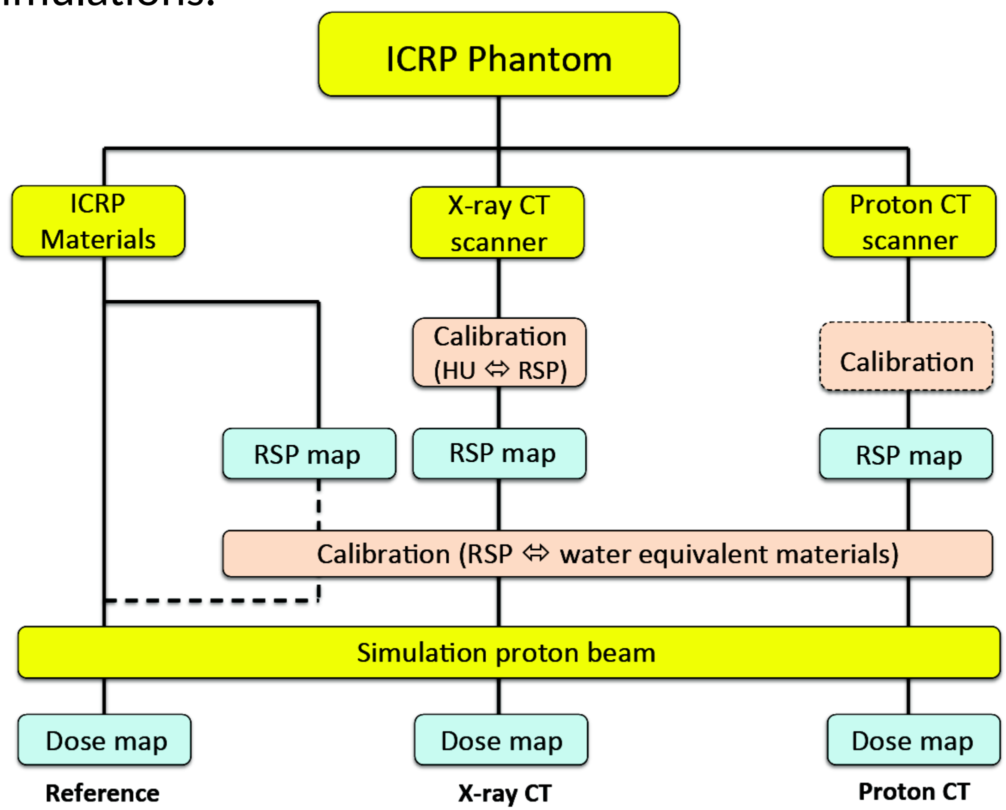

Monte Carlo Comparison of X-ray and Proton CT for Range Calculations of Proton Therapy Beams

Arbor et al., PMB 2015 in press

Imaging Dose

- Proton and X-ray CT images produced using a similar dose criterion based on patient volume that received 1 mGy or more (Dose-Volume Histogram)

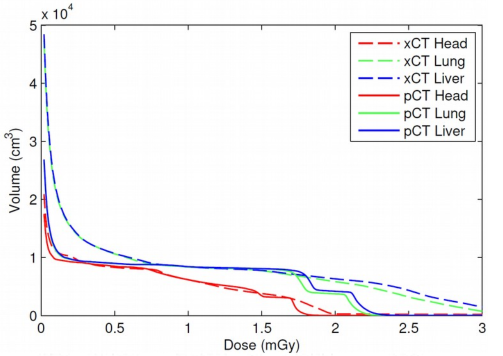

Dose-Volume Histogram for X-ray and proton CT

→ **Uniformity of proton dose distribution**

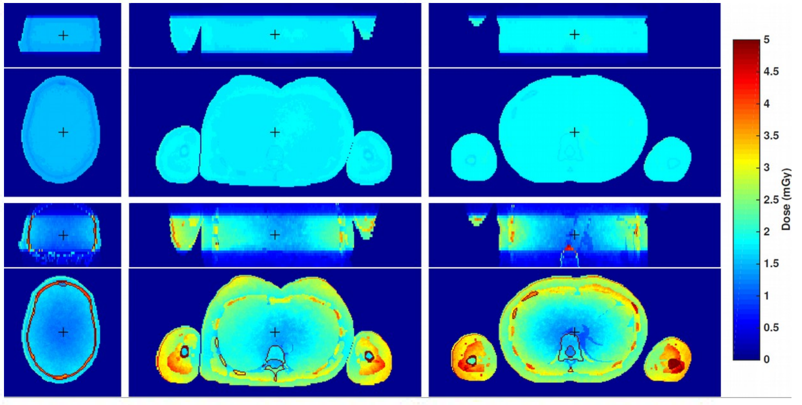

Image dose distribution for proton CT (top) and X-ray CT (bottom) [2]

Monte Carlo Comparison of X-ray and Proton CT for Range Calculations of Proton Therapy Beams

Arbor et al., PMB 2015 in press

RSP maps

- Apply X-ray and proton CT reconstruction to head, lungs and liver sites

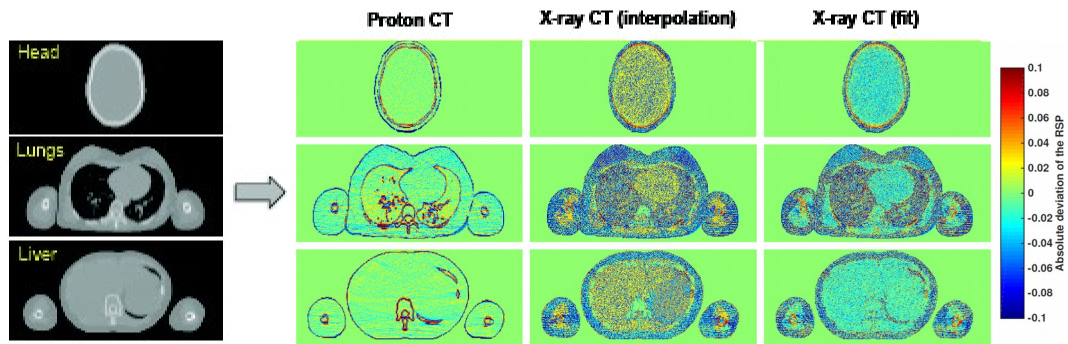

Proton CT RSP maps

RSP absolute deviation for proton and X-ray CT with respect to ICRP reference

- Compute voxel-by-voxel absolute deviation with respect to ICRP

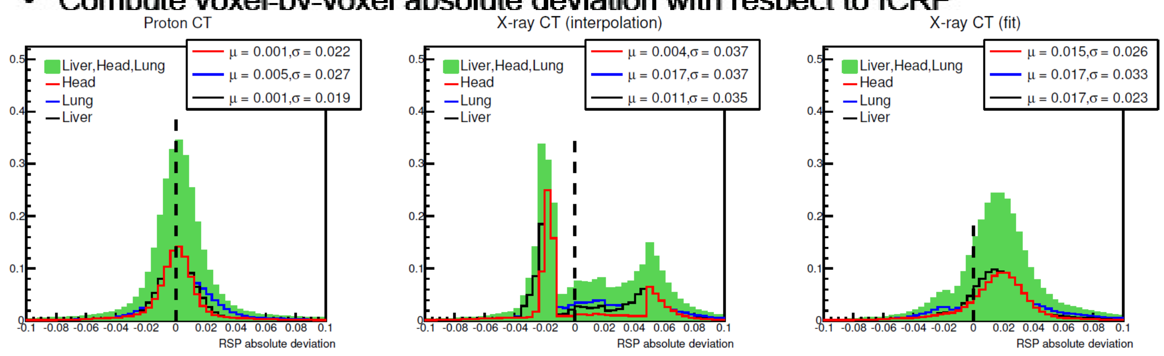

RSP absolute deviation for proton CT (left) and X-ray CT using linearly interpolated (middle) or least-square adjusted (right) calibration

Monte Carlo Comparison of X-ray and Proton CT for Range Calculations of Proton Therapy Beams

Arbor et al., PMB 2015 in press

Range calculations

- Transform RSP maps into water equivalent Monte Carlo materials
- Simulate proton beams (5 mm width) around patient
  (beam energy 100-140 MeV, mean proton range ≈ 120mm)
- Compute proton range deviation with respect to ICRP
  (Range defined as position with 80% dose maximum)

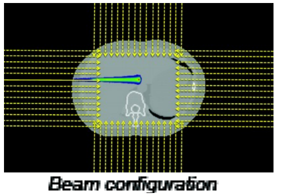

Beam configuration

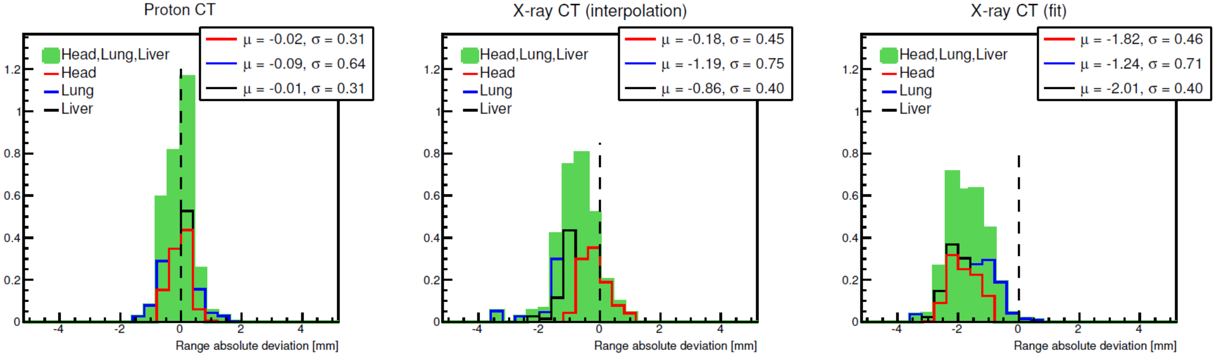

Range absolute deviation for proton CT (left) and X-ray CT using linearly interpolated (middle) or least-square adjusted (right) calibration

Conclusion

Using proton CT in proton therapy enables :
- a more uniform and conformal imaging dose distribution
- a more precise and more uniform accuracy of the tissues RSP
- a more precise calculation of the proton range

Present & Future

Technologies

- Proton Radiography with single energy proton beam

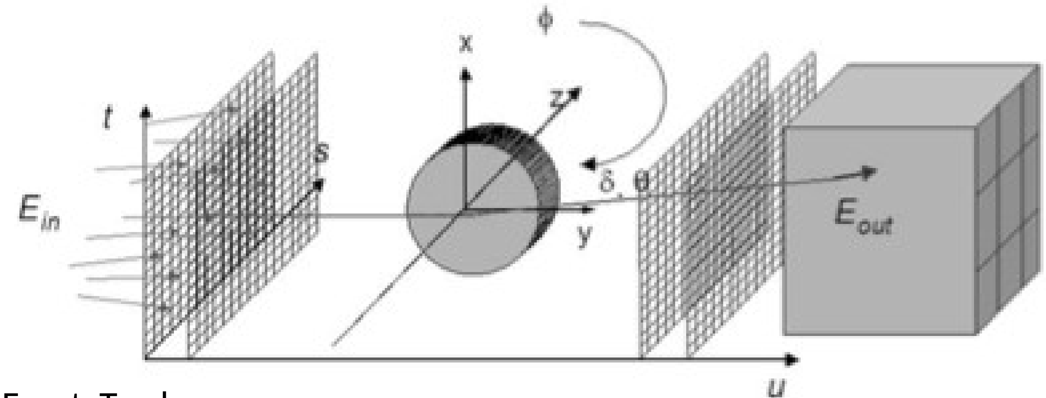

PSI: Schneider et. al. (2004)
LLUMC: Schulte et. al (2005)

Front Tracker - Hodoscope

Rear Tracker - Hodoscope

Calorimeter [LLUMC]
Range Telescope [PSI]

- Proton Radiography based on time-resolved dose measurements

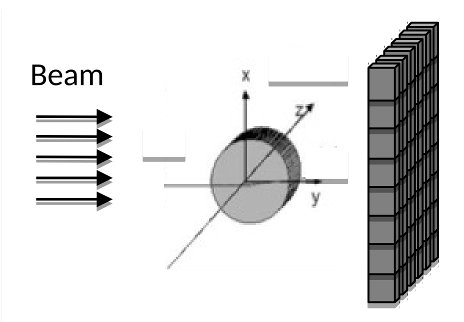

Dose Rate = E(t)

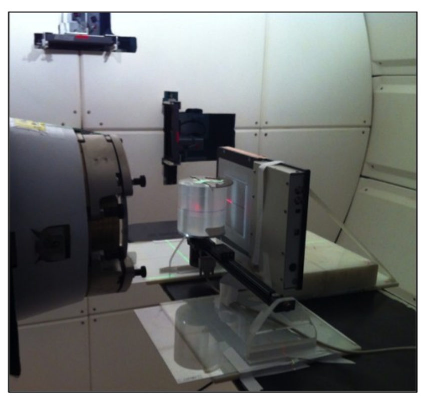

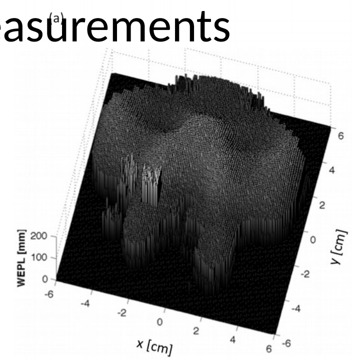

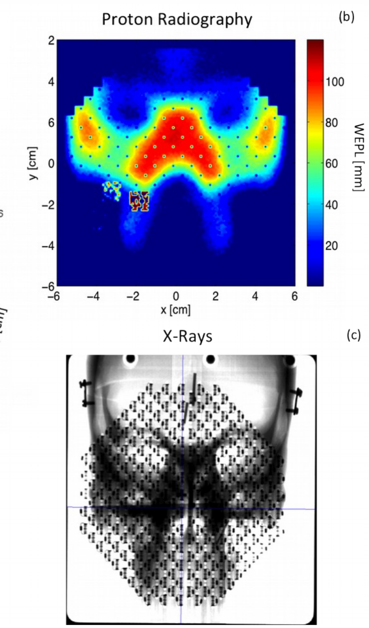

Testa et. al. PMB 2013

Experimental set-up

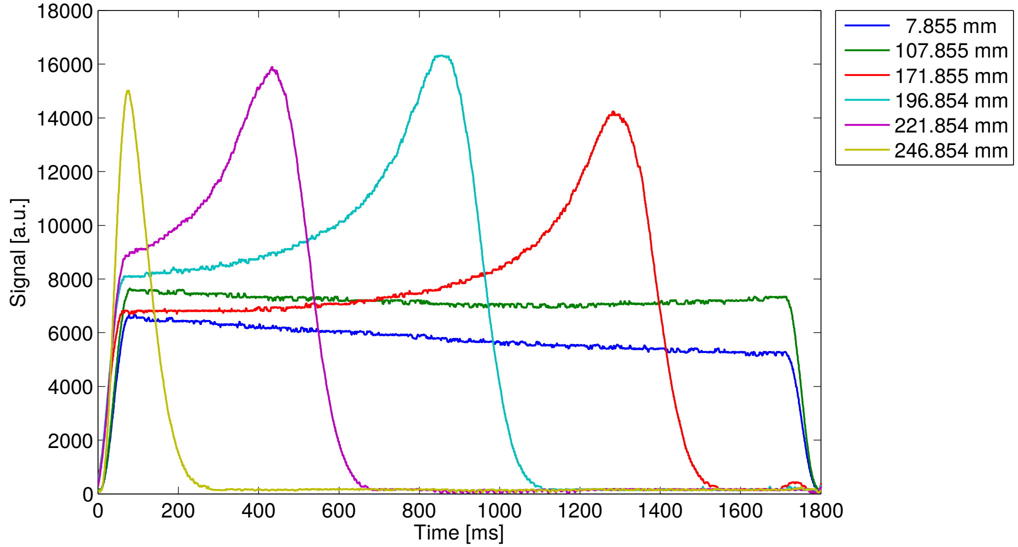

Scintillating Screen + CCD Camera

Range Modulator Wheel

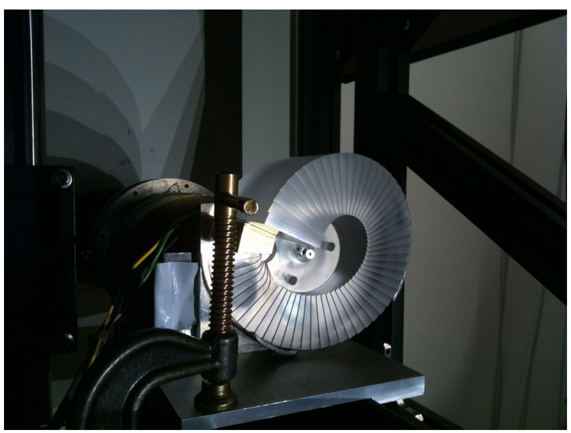

Technical Characteristics

Pixel size: 0.37 mm^2
Sampling Time: 120 ms
FOV: 30x30 cm^2

Wheel period: 20 s
Single Scattering
Modulation Width: 25cm

Conclusions of MGH Boston

- Time-resolved proton radiography is a promising technique:
  - No need of bulky detection system (trackers – single proton counting – Range telescopes (IC-stacks) or Calorimeters (very complex to calibrate)
  - Single plane detector only (compact)
  - Image formed simultaneously over the whole FOV (0.1 s – 1.8s – 20s)
- Compact system potentially applicable to scanning beam-lines with external dedicated RMW
- Detector:
  - Trade-off between space resolution and detection efficiency (diode *vs*. scintillating screens 0.7 - 3 cGy)
  - Trade-off between RMW period and detector sampling time
- Still (a lot) of work to do on new reconstruction algorithms

What we need to make experiments

- Range Modulator Wheel (Scatterer + Modulation)
- Step-Motor

- Detector
  - BIS – Lynx IBA (high dose per radiography)
  - Fluoroscopy x-ray panel (low dose per radiography)

- Ion Chamber in water phantom to measure SOBP capable of measuring DRF

- Phantoms and access to CT to produce DRR

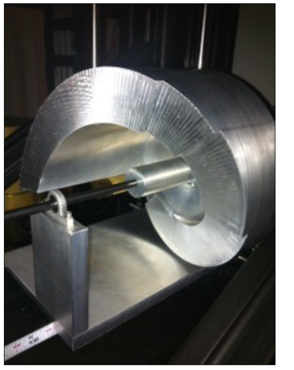

Thank you

Results: Step-Phantom

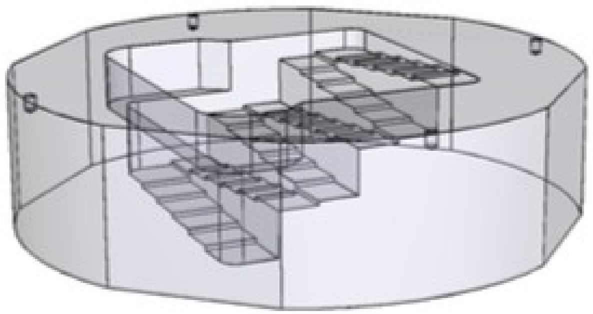

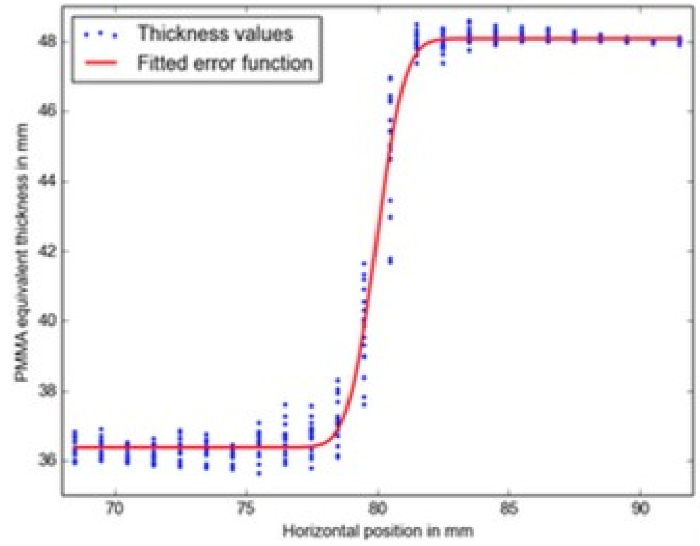

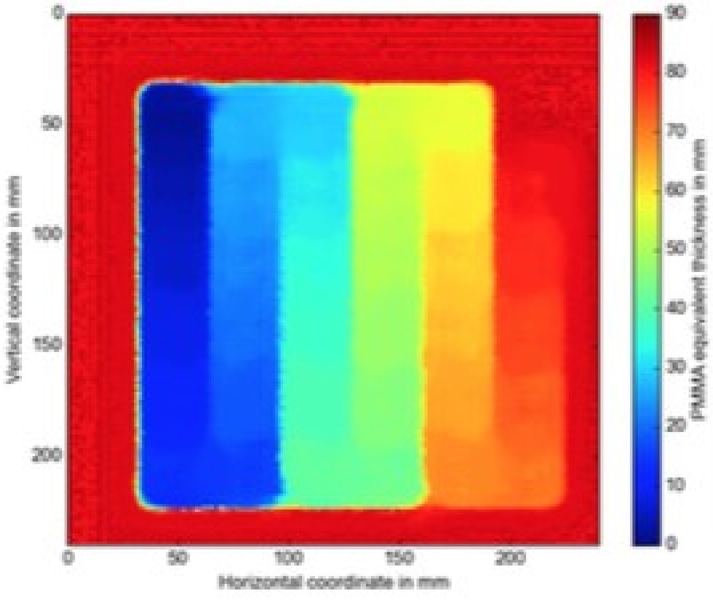

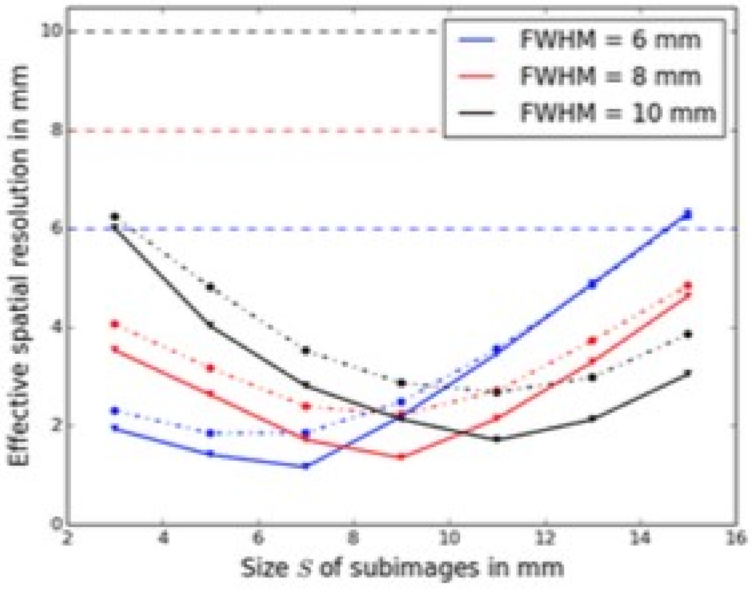

Step 2. Sub-images

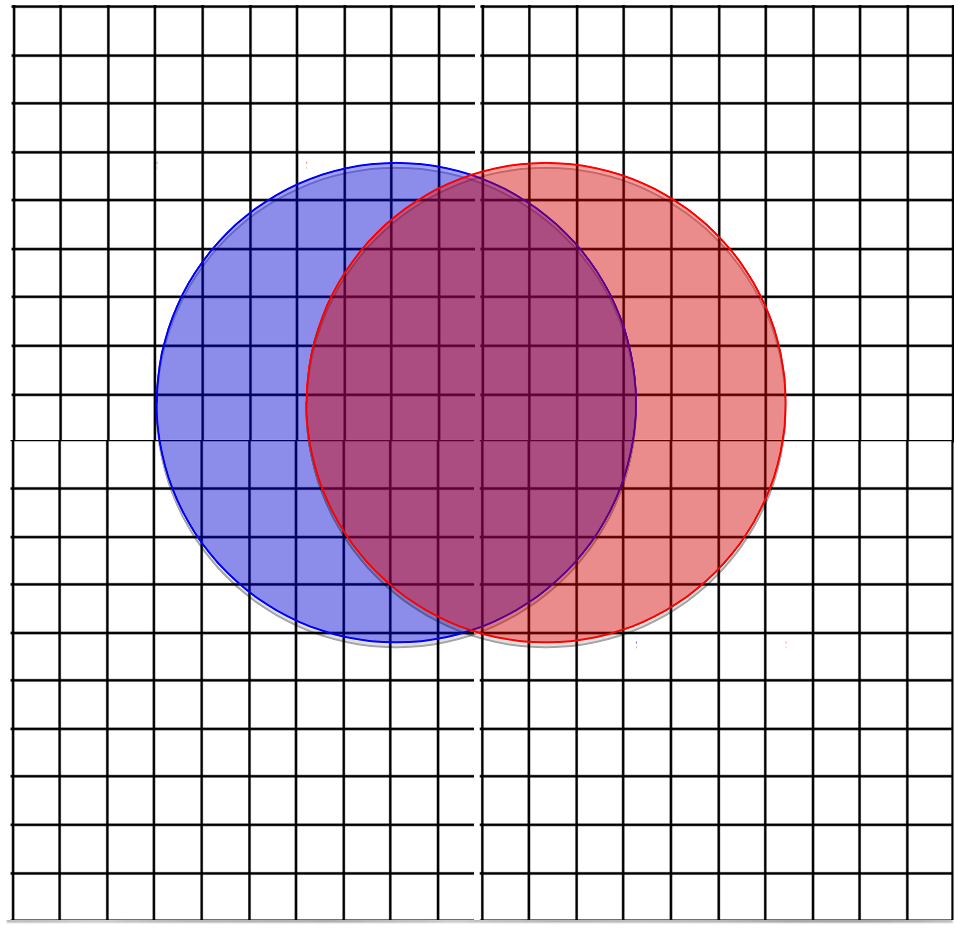

Image pixel size: 1mm
FWHM beam: 8mm
Step-size raster scanning: 1mm

Step 2. Sub-images

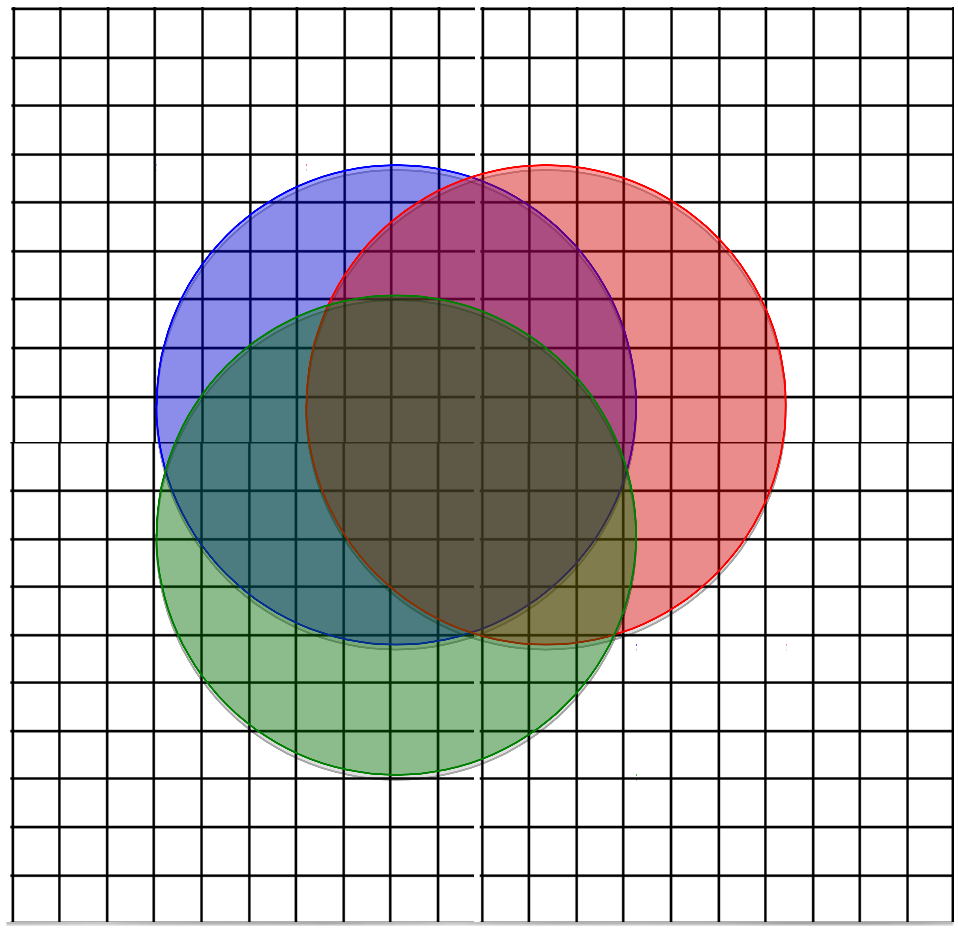

Image pixel size: 1mm
FWHM beam: 8mm
Step-size raster scanning: 1mm